Mathematics

https://www.aimspress.com/journal/Math

AIMS Mathematics, 11(6): 16570–16601.
DOI: 10.3934/math.2026680
Received: 09 March 2026
Revised: 20 May 2026
Accepted: 28 May 2026
Published: 09 June 2026

Research article

The Riemann problem and wave interactions for a relativistic p-system with variable heat ratios

Jiatao Yao and Qinglong Zhang*

School of Mathematics and Statistics, Ningbo University, 315211, China

* **Correspondence:** Email: zhangqinglong@nbu.edu.cn.

Abstract: We comprehensively investigate the Riemann problem for a relativistic p-system with variable heat ratios. First, we consider the relativistic system when the heat ratio γ changes. We supplement with the trivial equation $\frac{\partial}{\partial t}\gamma = 0$ to close the system. Second, we solve the Riemann problem with piecewise constant of heat ratios, and obtain the elementary waves, including rarefaction waves, shock waves, contact discontinuities, and particularly stationary waves. An admissible stationary wave selection method based on monotone criterion is studied. Finally, we discuss the interaction of elementary waves, particularly, rarefaction wave and shock wave interactions with stationary wave, respectively. The large-time behavior of each case is also presented.

Keywords: the Riemann problem; relativistic system; variable heat ratios; stationary wave; wave interactions
Mathematics Subject Classification: 35L65, 35L80, 35R35

1. Introduction

Considering the system of conservation laws in energy and momentum in special relativity, Smoller and Temple obtained the form of the one-dimensional relativistic Euler system (namely, (23), (25), and (26) in [1]),

$$\begin{cases} \dfrac{\partial}{\partial t}\left((p+\rho c^2)\dfrac{v^2}{c^2-v^2}\right)+\dfrac{\partial}{\partial x}\left((p+\rho c^2)\dfrac{v^2}{c^2-v^2}+p\right)=0, \\ \dfrac{\partial}{\partial t}\left(\dfrac{(p+\rho c^2)}{c^2}\dfrac{v^2}{c^2-v^2}+\rho\right)+\dfrac{\partial}{\partial x}\left((p+\rho c^2)\dfrac{v}{c^2-v^2}\right)=0, \end{cases} \tag{1.1}$$

where c is the speed of light, ρ is the proper energy density, p is the pressure, and v is the particle speed. For convenience, we take the speed of light $c = 1$. Then, the system reduces to

$$\begin{cases} \dfrac{\partial}{\partial t}\left((\rho + p)\dfrac{v}{1 - v^2}\right) + \dfrac{\partial}{\partial x}\left((\rho + p)\dfrac{v^2}{1 - v^2} + p\right) = 0, \\ \dfrac{\partial}{\partial t}\left((\rho + p)\dfrac{v^2}{1 - v^2} + \rho\right) + \dfrac{\partial}{\partial x}\left((\rho + p)\dfrac{v}{1 - v^2}\right) = 0, \end{cases} \tag{1.2}$$

where the equation of state $p = p(\rho) = k\rho^\gamma$ is a smooth function of ρ and satisfies $p'(\rho) > 0$, $p''(\rho) \geq 0$, k is a positive constant, and γ is the ratio of specific heats. Since all speeds are less than the speed of light, we need to bound the speed of sound by the speed of light, i.e., $\sqrt{p'(\rho)} < 1$; see [2]. Taub [3, 4] then obtained that the Hugoniot curve of relativistic shocks, and also showed that γ must satisfy $1 < \gamma < \frac{5}{3}$. As far as we know, the ratio γ has been treated as a constant in previous research, so the system is considered under thermostatic circumstances. As showed in [5], for a monatomic relativistic gas, γ is a function of temperature, starting at $\frac{5}{3}$ in the low-temperature limit and decreasing monotonically to the high-temperature limit of $\frac{4}{3}$. In this article, we focus on the relativistic system with variable heat ratios, i.e., γ can be treated as a variable.

In order to investigate the relativistic fluid dynamics in variable heats, we introduce the following trivial equation, given by

$$\frac{\partial}{\partial t}\gamma = 0 \tag{1.3}$$

to close the system. This condition means that γ is independent of time, which is similar to [6, 7] where the cross section area $a(x)$ is given as a function of x. Thus, we assume that the adiabatic index γ is a function of x and does not change with time. Other choices of γ may also be chosen and will not be considered here.

In this paper, we study the Riemann problem associated with (1.2) and (1.3), where the initial data is given by the two piecewise constants,

$$(\rho, v, \gamma) = \begin{cases} (\rho_L, v_L, \gamma_L), & x < 0, \\ (\rho_R, v_R, \gamma_R), & x > 0. \end{cases} \tag{1.4}$$

Since the system under investigation is not strictly hyperbolic, we recall some results of non-strictly hyperbolic systems, which have attracted much interest both theoretically and numerically in recent years. LeFloch and Thanh [8] constructed the Riemann solutions for the model of isentropic flows in a nozzle with variable cross-section. They also extend the method to the shallow water system [9]. Andrianov and Warnecke [10] also considered the Riemann problem in a different way, and they introduced a new concept of solutions. They further solved the Riemann problem for a two-phase flow model constructively in [11].

Inspired by these mathematical models and methods, we aim to construct the Riemann solutions for the relativistic p-system with variable heat ratios. However, compared to the duct flows or the shallow water equations, there is a fundamental difference of (1.2) with (1.3), i.e., the speed of sound $\sqrt{p'(\rho)}$ depends on the variable heat ratios γ, so that the characteristic fields bring difficulties to define the sonic curve as γ changes.

Since Taub's fundamental work, the theory of relativistic fluid dynamics has made great progress. Makino [12], and Chen and Li [13, 14] extended their results to the more general case $p = p(\rho)$. More recently, Wissman [15] had extended Smoller and Temple's result to the 1-D full relativistic Euler equations with the equation of state $p = \sigma^2\rho$. Lai [16] investigated the self-similar solutions of the radially symmetric relativistic equations. Yin and Sheng [17] investigated the vanishing pressure limit of the Riemann solutions for the relativistic Euler system with polytropic gases. Zhang and Yang [18] studied the flux approximation problem for the relativistic Euler equations in special relativity. The concentration and cavitation in the vanishing pressure limit are studied in [19]. Numerical solutions are also available in [20–22]. In this paper, we focus on the Riemann problem for (1.2) and (1.3), and the stationary wave is carefully used to construct the solutions. In order to ensure the uniqueness of stationary solutions, we also introduce the admissibility criterion on stationary wave based on the monotone criterion. Resonance and coalescence of waves are also analyzed. The interactions of rarefaction waves and shock waves with stationary waves are also discussed in the paper.

The organization of this paper is as follows. In Section 2, we conduct a characteristic analysis for systems (1.2) and (1.3), and the elementary waves of this system are introduced, including rarefaction waves, shock waves, contact discontinuities, and stationary waves. An admissibility criterion is proposed to ensure the uniqueness of the stationary wave. In Section 3, we construct the Riemann solutions for a relativistic p-system with variable heat ratios systematically. The resonance phenomenons are discussed. In Section 4, we consider the interactions of rarefaction waves and shock waves with the stationary waves, respectively, and the large-time behaviors are obtained in each case.

2. Characteristic analysis and elementary waves for (1.2) and (1.3)

2.1. Preliminaries

The complete system is

$$\begin{cases} \dfrac{\partial}{\partial t}\left((\rho+p)\,\dfrac{v}{1-v^2}\right)+\dfrac{\partial}{\partial x}\left((\rho+p)\,\dfrac{v^2}{1-v^2}+p\right)=0, \\ \dfrac{\partial}{\partial t}\left((\rho+p)\,\dfrac{v^2}{1-v^2}+\rho\right)+\dfrac{\partial}{\partial x}\left((\rho+p)\,\dfrac{v}{1-v^2}\right)=0, \\ \dfrac{\partial}{\partial t}\gamma=0, \quad x\in R, t>0, \end{cases} \tag{2.1}$$

where the pressure $p = k\rho^\gamma$, $1 < \gamma < \frac{5}{3}$, and k is a positive constant. Denote $U = (\rho, v, \gamma)$. Considering a smooth solution, we can rewrite system (2.1) as

$$A(U)\partial_t U + B(U)\partial_x U = 0, \tag{2.2}$$

where

$$A=\begin{pmatrix} (1+p_\rho)\frac{v}{1-v^2} & (\rho+p)\frac{1+v^2}{(1-v^2)^2} & p_\gamma\frac{v}{1-v^2} \\ (1+p_\rho)\frac{v^2}{1-v^2}+1 & (\rho+p)\frac{2v}{(1-v^2)^2} & p_\gamma\frac{v^2}{1-v^2} \\ 0 & 0 & 1 \end{pmatrix},$$

$$B=\begin{pmatrix} \left(1+p_\rho\right)\frac{v^2}{1-v^2}+p_\rho & (\rho+p)\,\frac{2v}{\left(1-v^2\right)^2} & \frac{p_\gamma}{1-v^2} \\ \left(1+p_\rho\right)\frac{v}{1-v^2} & (\rho+p)\,\frac{1+v^2}{\left(1-v^2\right)^2} & p_\rho\frac{v}{1-v^2} \\ 0 & 0 & 0 \end{pmatrix}. \tag{2.3}$$

The Jacobian matrix of (2.1) is

$$J = A^{-1}B = \begin{pmatrix} \frac{v(1-p_\rho)}{1-v^2p_\rho} & \frac{\rho+p}{1-v^2p_\rho} & -\frac{vp_\rho}{1-v^2p_\rho} \\ \frac{p_\rho(1-v^2)^2}{(\rho+p)(1-v^2p_\rho)} & \frac{v(1-p_\rho)}{1-v^2p_\rho} & \frac{p_\rho(1-v^2)}{(\rho+p)(1-v^2p_\rho)} \\ 0 & 0 & 0 \end{pmatrix}. \tag{2.4}$$

Thus, the eigenvalues of (2.2) are determined by $|J-\lambda I| = 0$, which yields the eigenvalues

$$\lambda_1 = \frac{v-\sqrt{p_\rho}}{1-v\sqrt{p_\rho}}, \quad \lambda_2 = \frac{v+\sqrt{p_\rho}}{1+v\sqrt{p_\rho}}, \quad \lambda_3 = 0. \tag{2.5}$$

The corresponding right eigenvectors can be chosen as

$$r_1 = (1, \frac{\sqrt{p_\rho}\left(v^2-1\right)}{\rho+p}, 0)^t, r_2 = (1, \frac{\sqrt{p_\rho}\left(1-v^2\right)}{\rho+p}, 0)^t, r_3 = (1, \frac{v\left(v^2-1\right)}{\rho+p}, \frac{v^2-p_\rho}{p_\rho})^t. \tag{2.6}$$

We have

$$\begin{aligned} \nabla\lambda_1 &= \left(\partial_\rho\lambda_1, \partial_v\lambda_1, \partial_\gamma\lambda_1\right) \\ &= \left(-\frac{1}{2}\frac{\frac{\partial^2 p}{\partial\rho^2}}{\left(1-v\sqrt{p_\rho}\right)^2\sqrt{p_\rho}}, \frac{1-p_\rho}{\left(1-v^2\sqrt{p_\rho}\right)^2}, -\frac{1}{2}\frac{\frac{\partial^2 p}{\partial\gamma\partial\rho}\left(1-v^2\right)}{\left(1-v\sqrt{p_\rho}\right)^2\sqrt{p_\rho}}\right). \end{aligned} \tag{2.7}$$

Then we find that

$$\nabla\lambda_1\cdot r_1 = -\frac{1}{2}\left(1-v^2\right)\frac{\frac{\partial^2 p}{\partial\rho^2}(\rho+p)+2\sqrt{p_\rho}\left(1-p_\rho\right)}{\left(1-v\sqrt{p_\rho}\right)^2\sqrt{p_\rho}(\rho+p)} < 0, \tag{2.8}$$

i.e., $\nabla\lambda_1\cdot r_1$ is always negative. Thus, λ_1 is genuinely nonlinear. Similarly, we can prove that λ_2 is genuinely nonlinear and $\nabla\lambda_3\cdot r_3 = 0$ so that λ_3 is linearly degenerate. System (2.1) is non-strictly hyperbolic since λ_1 and λ_2 can coincide with λ_3. In the (ρ, v, γ)-space, there are two surfaces, denoted by Γ_+ and Γ_-, on which the system fails to be hyperbolic:

$$\begin{aligned} \Gamma_+ :&= \{U = (\rho, v, \gamma) : \lambda_3(U) = \lambda_1(U)\} \\ &= \left\{(\rho, v, \gamma) : v = \sqrt{p_\rho}\right\}, \\ \Gamma_- :&= \{U = (\rho, v, \gamma) : \lambda_3(U) = \lambda_2(U)\} \\ &= \left\{(\rho, v, \gamma) : v = -\sqrt{p_\rho}\right\}. \end{aligned}$$

Γ_+ and Γ_- separate the phase domain into three subdomains, denoted by D_1, D_2, and D_3, in which the system is strictly hyperbolic (see Figure 1):

$$D_1 = \{(\rho, v)\,|\lambda_3(U) < \lambda_1(U) < \lambda_2(U)\},$$

$$D_2 = \{(\rho, v)\,|\lambda_1(U) < \lambda_3(U) < \lambda_2(U)\},$$

$$D_3 = \{(\rho, v)\,|\lambda_1(U) < \lambda_2(U) < \lambda_3(U)\}.$$

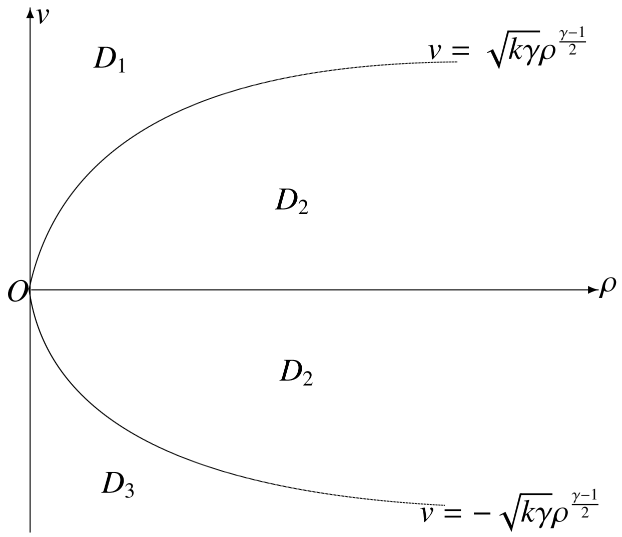

Figure 1. Projection of strictly hyperbolic subdomains in the (ρ, v)-plane.

2.2. The rarefaction waves

There are two families of rarefaction waves in the characteristic fields corresponding to λ_1 and λ_2, respectively. A rarefaction wave is a continuous solution of (1.2) with the form

$$U(x,t) = U(\xi), \quad \xi = x/t.$$

The Riemann invariant w_i corresponding to λ_i should satisfy

$$\nabla w_i \cdot r_i = 0, \quad i = 1, 2.$$

For λ_1, $\nabla w_1 \cdot r_1 = 0$ is equivalent to

$$(w_1)_\rho - (w_1)_v \frac{\sqrt{p_\rho}(1-v^2)}{\rho + p} = 0. \tag{2.9}$$

It can be found that $w_1 = \gamma$ is a trivial solution satisfying (2.9). Otherwise, w_1 remains invariant along the direction

$$\frac{\mathrm{d}v}{\mathrm{d}\rho} = -\frac{\sqrt{p_\rho}\left(1-v^2\right)}{\rho + p}. \tag{2.10}$$

We find that

$$\frac{1}{2}\ln\left(\frac{1+v}{1-v}\right) + \int \frac{\sqrt{p_\rho}}{\rho + p}\mathrm{d}\rho = \text{const}. \tag{2.11}$$

Thus, the Riemann invariants along the λ_1 characteristic field are

$$w_1^1 = \frac{1}{2}\ln\left(\frac{1+v}{1-v}\right) + \int \frac{\sqrt{p_\rho}}{\rho + p}\mathrm{d}\rho, \quad w_1^2 = \gamma. \tag{2.12}$$

Similarly, the Riemann invariants along the λ_2 characteristic field are

$$w_2^1 = \frac{1}{2}\ln\left(\frac{1+v}{1-v}\right) - \int \frac{\sqrt{p_\rho}}{\rho + p}\mathrm{d}\rho, \quad w_2^2 = \gamma. \tag{2.13}$$

We find that γ remains constant across the rarefaction waves. Given the left-hand state U_0, the backward 1-rarefaction curve $R_1(U_0, U)$ connected to the right-hand states U is given by

$$R_1(U_0, U) : \frac{1}{2}\ln\left(\frac{1+v}{1-v}\right) - \frac{1}{2}\ln\left(\frac{1+v_0}{1-v_0}\right) = \int_{\rho_0}^{\rho} \frac{-\sqrt{p'(z)}}{z+p(z)}\mathrm{d}z, \quad 0 < \rho < \rho_0. \tag{2.14}$$

Moreover, given the right-hand state U_0, the forward 2-rarefaction curve $R_2(U, U_0)$ connected to the left-hand states U is given by

$$R_2(U, U_0) : \frac{1}{2}\ln\left(\frac{1+v}{1-v}\right) - \frac{1}{2}\ln\left(\frac{1+v_0}{1-v_0}\right) = \int_{\rho_0}^{\rho} \frac{\sqrt{p'(z)}}{z+p(z)}\mathrm{d}z, \quad 0 < \rho < \rho_0. \tag{2.15}$$

2.3. The discontinuity solutions

The Rankine-Hugoniot relation associated with (1.3) is

$$-\sigma[\gamma] = 0,$$

where $[\gamma] := \gamma_+ - \gamma_-$ is the jump of the ratio γ. We have the following conclusions:

(i) $[\gamma] = 0$: the component γ remains constants across the non-zero speed shocks.
(ii) $\sigma = 0$: the shock speed vanishes, here we assume $[\gamma] \neq 0$, and call it stationary contact discontinuity.

2.3.1. The shock waves

Let us first consider case (i). The Rankine-Hugoniot conditions corresponding to (1.2) are given by

$$\begin{cases} \sigma[(\rho+p)\dfrac{v}{1-v^2}] = [(\rho+p)\dfrac{v^2}{1-v^2} + p], \\ \sigma[(\rho+p)\dfrac{v^2}{1-v^2} + \rho] = [(\rho+p)\dfrac{v}{1-v^2}], \end{cases} \tag{2.16}$$

where $[f] = f_+ - f_-$ is the jump of the function of f, and σ is the speed of propagation of the discontinuity connecting the left-hand state U_0 and the right-hand state U.

By eliminating σ, we get

$$\frac{(\rho+p)\frac{v^2}{1-v^2} + \rho - (\rho_0+p_0)\frac{v_0^2}{1-v_0^2} - \rho_0}{(\rho+p)\frac{v}{1-v^2} - (\rho_0+p_0)\frac{v_0}{1-v_0^2}} = \frac{(\rho+p)\frac{v}{1-v^2} - (\rho_0+p_0)\frac{v_0}{1-v_0^2}}{(\rho+p)\frac{v^2}{1-v^2} + p - (\rho_0+p_0)\frac{v_0^2}{1-v_0^2} - p_0}. \tag{2.17}$$

Thus, we have

$$\frac{(v-v_0)^2}{(1-v^2)\left(1-v_0^2\right)} = \frac{(p-p_0)(\rho-\rho_0)}{(\rho+p)(\rho_0+p_0)}. \tag{2.18}$$

The shock waves of (2.16) associated with nonlinear characteristic fields must satisfy the Lax entropy conditions

$$\lambda_i(U) < \sigma(U_0, U) < \lambda_i(U_0), \quad i = 1, 2. \tag{2.19}$$

The Lax shock conditions are equivalent to

(i) For a 1-shock,

$$\rho > \rho_0, \quad v < v_0. \tag{2.20}$$

(ii) For a 2-shock,

$$\rho < \rho_0, \quad v < v_0. \tag{2.21}$$

Thus, for a non-zero speed shock wave, given a left-hand state U_0, the backward 1-shock curve $S_1(U_0, U)$ consisting of the right-hand states U is determined by

$$S_1(U_0, U): \frac{v - v_0}{\sqrt{(1 - v^2)\left(1 - v_0^2\right)}} = -\sqrt{\frac{(p - p_0)(\rho - \rho_0)}{(\rho + p)(\rho_0 + p_0)}}, \quad \rho > \rho_0. \tag{2.22}$$

Similarly, given a right-hand state U_0, the inequalities in (2.21) must be reversed, and the forward 2-shock curve $S_2(U, U_0)$ consisting of the left-hand states U is determined by

$$S_2(U, U_0): \frac{v - v_0}{\sqrt{(1 - v^2)\left(1 - v_0^2\right)}} = \sqrt{\frac{(p - p_0)(\rho - \rho_0)}{(\rho + p)(\rho_0 + p_0)}}, \quad \rho > \rho_0. \tag{2.23}$$

For convenience, we can define the wave curve as follows:

$$W_1(U_0, U) := S_1(U_0, U) \cup R_1(U_0, U), \quad W_2(U, U_0) := S_2(U, U_0) \cup R_2(U, U_0).$$

Now we explore some properties of the wave curves.

Lemma 2.1. *The wave curve $W_1(U_0, U)$ can be parameterized in the form $\rho \mapsto v = v(\rho)$, where the function $v(\rho)$ is monotone decreasing in ρ. The wave curve $W_2(U, U_0)$ can be parameterized in the form $\rho \mapsto v = v(\rho)$, where the function $v(\rho)$ is monotone increasing in ρ.*

Proof. We only give the proof for the 1-wave curve $W_1(U_0, U)$, and the proof for $W_2(U, U_0)$ is similar. For the shock wave $S_1(U_0, U)$, by differentiating (2.18) on each side with respect to ρ, we obtain

$$\begin{aligned} &\frac{2(v - v_0)\frac{dv}{d\rho}(1 - v^2)^2(1 - v_0^2)^2 - (v - v_0^2)(-2v)\frac{dv}{d\rho}(1 - v_0^2)}{(1 - v^2)^2(1 - v_0^2)^2} \\ &= \frac{\left[p'(\rho)(\rho - \rho_0) + (p - p_0)\right](\rho + p) - (p - p_0)(\rho - \rho_0)\left[p'(\rho) + 1\right]}{(\rho + p)^2(\rho_0 + p_0)}. \end{aligned} \tag{2.24}$$

Thus, we get

$$\frac{dv}{d\rho} = \frac{\left[p'(\rho)(\rho - \rho_0)(p_0 + \rho) + (p - p_0)(p + \rho_0)\right](1 - v^2)^2(1 - v_0^2)}{2(\rho + p)^2(\rho_0 + p_0)(v - v_0)(1 - v v_0)} < 0 \tag{2.25}$$

along the 1-shock wave curve.

For the rarefaction wave $R_1(U_0, U)$, from (2.14) we have

$$\frac{dv}{d\rho} = -\frac{\sqrt{p'(\rho)}(1 - v^2)}{\rho + p} < 0 \tag{2.26}$$

along the 1-rarefaction wave curve. Thus, we prove the properties of $W_1(U_0, U)$. □

2.3.2. The stationary contact discontinuities

In this part, we discuss the stationary contact discontinuities (case (ii)). As in LeFloch and Thanh [8], a stationary solution is a time-independent smooth solution. Thus, we consider the following ordinary differential equations:

$$\begin{cases} \left((\rho + p) \dfrac{v^2}{1 - v^2} + p \right)' = 0, \\ \left((\rho + p) \dfrac{v}{1 - v^2} \right)' = 0, \end{cases} \tag{2.27}$$

where f' denotes $\frac{\mathrm{d}f}{\mathrm{d}x}$.

First, we define

$$\begin{cases} (\rho + p) \dfrac{v}{1 - v^2} = (\rho_0 + p_0) \dfrac{v_0}{1 - v_0^2} := M, \\ (\rho + p) \dfrac{v^2}{1 - v^2} + p = (\rho_0 + p_0) \dfrac{v_0^2}{1 - v_0^2} + p_0 := N, \end{cases} \tag{2.28}$$

where U_0 is the given left-hand state, and U is the right-hand state of the stationary discontinuity, and $p = k\rho^\gamma$, $p_0 = k\rho^{\gamma_0}$, and $\gamma \neq \gamma_0$. This yields

$$v = \frac{Mv_0 + p_0 - p}{M} = \frac{Mv_0 + p_0 - k\rho^\gamma}{M}, \tag{2.29}$$

$$M^2 - N^2 = \frac{v_0^2 \rho_0^2 - p_0^2}{1 - v_0^2} = \frac{v^2 \rho^2 - p^2}{1 - v^2}. \tag{2.30}$$

Substituting (2.29) into (2.28), we get

$$(\rho + k\rho^\gamma) \frac{\frac{Mv_0 + p_0 - k\rho^\gamma}{M}}{1 - \left(\frac{Mv_0 + p_0 - k\rho^\gamma}{M} \right)^2} = (\rho_0 + p_0) \frac{v_0}{1 - v_0^2} = M. \tag{2.31}$$

After arranging the terms, we obtain

$$F(\rho, \gamma; U_0) := k\rho^{\gamma+1} + kN\rho^\gamma - N\rho + M^2 - N^2 = 0. \tag{2.32}$$

It is obvious that

$$\lim_{\rho \to 0} F(\rho, \gamma; U_0) = M^2 - N^2, \quad \lim_{\rho \to 1} F(\rho, \gamma; U_0) = k + kN - N + M^2 - N^2. \tag{2.33}$$

Thus, we conclude that if $v_0^2 \rho_0^2 - p_0^2 > 0$, then $\lim_{\rho \to 0} F(\rho, \gamma; U_0) > 0$; if $v_0^2 \rho_0^2 - p_0^2 < 0$, then $\lim_{\rho \to 0} F(\rho, \gamma; U_0) < 0$. Here, we assume $\lim_{\rho \to 0} F(\rho, \gamma; U_0) > 0$ (for example, $k > 1$), and the other case can be discussed similarly.

Furthermore, we have

$$\frac{\mathrm{d}F(\rho, \gamma; U_0)}{\mathrm{d}\rho} = k(\gamma + 1)\rho^\gamma + k\gamma N\rho^{\gamma-1} - N. \tag{2.34}$$

Then,

$$\lim_{\rho\to 0}\frac{\mathrm{d}F(\rho,\gamma;U_0)}{\mathrm{d}\rho}=-N<0,\quad \lim_{\rho\to 1}\frac{\mathrm{d}F(\rho,\gamma;U_0)}{\mathrm{d}\rho}=k(\gamma+1)+k\gamma N-N>0, \tag{2.35}$$

$$\frac{\mathrm{d}^2F(\rho,\gamma;U_0)}{\mathrm{d}\rho^2}=k\gamma(\gamma+1)\rho^{\gamma-1}+k\gamma(\gamma-1)N\rho^{\gamma-2}>0. \tag{2.36}$$

Thus,

$$\frac{\mathrm{d}F(\rho,\gamma;U_0)}{\mathrm{d}\rho}\begin{cases}<0, & \text{if } \rho<\rho_{min},\\ >0, & \text{if } \rho>\rho_{min},\end{cases} \tag{2.37}$$

where ρ_{min} satisfies $F'(\rho_{min})=0$.

Moreover, we know that both M and N are determined by $U_0(\rho_0,v_0,\gamma_0)$ and γ. In other words, if $U_0(\rho_0,v_0,\gamma_0)$ is fixed, then ρ_{min} only depends on γ. From (2.33), (2.32) admits a solution if and only if

$$F(\rho_{min})\le 0.$$

Lemma 2.2 (stationary contact discontinuity)**.** *Given the left-hand state $U_0(\rho_0,v_0,\gamma_0)$, there is a stationary contact discontinuity connecting to the right-hand state $U(\rho,v,\gamma)$ if and only if $F(\rho_{min})\le 0$. More precisely, we have the following:*

(i) If $F(\rho_{min})>0$, there are no stationary contacts.

(ii) If $F(\rho_{min})\le 0$, then

(a) if $v_0^2\rho_0^2-p_0^2>0$, there are exactly two points $U_*=(\rho_*,v_*,\gamma)$, $U^*=(\rho^*,v^*,\gamma)$, where $\rho_*(U_0,\gamma)<\rho_{min}(U_0)<\rho^*(U_0,\gamma)$ satisfies

$$F(\rho_*;U_0)=F(\rho^*;U_0)=0. \tag{2.38}$$

The two values U_* and U^* coincide if and only if $F(\rho_{min})=0$.

(b) if $v_0^2\rho_0^2-p_0^2\le 0$, there is only one point $\hat{U}=(\hat{\rho},\hat{v},\gamma)$ satisfying

$$F(\hat{\rho};U_0)=0. \tag{2.39}$$

As shown in [7, 23], the Riemann problem for (2.1) may admit up to a one-parameter family of solutions. This phenomenon can be avoided by requiring Riemann solutions to satisfy an admissibility criterion: monotone condition on the component γ. In order to determine the unique solution of the stationary contact, it is necessary to impose an additional admissibility criterion.

Admissibility criterion. Along the stationary curve in the (ρ,v)-plane between the left and right-hand states of any stationary wave, the component γ obtained from (2.32) is a monotone function of ρ along the stationary curve $S_0(U_0,U)$.

Under the transformation

$$x\longmapsto -x,\quad v\longmapsto -v,$$

a right-hand state $U(\rho,v,\gamma)$ can be transformed into a left-hand state $U(\rho,-v,\gamma)$. Without loss of generality, we assume γ is an increasing function of ρ, i.e., $\gamma_R>\gamma_L$.

In order to analyze stationary wave clearly, we need to denote the following surfaces:

$$\Sigma_1: v=\sqrt{k\gamma}\rho^{\frac{\gamma-1}{2}},\quad \Sigma_2: v=k\rho^{\gamma-1},$$

$$\Sigma_3 : v = 0, \quad \Sigma_4 : v = -k\rho^{\gamma-1}, \quad \Sigma_5 : v = -\sqrt{k\gamma}\rho^{\frac{\gamma-1}{2}}.$$

The (ρ, v, γ)-space is separated by these surfaces into six subdomains, denoted by $G_i, i = 1, 2, \cdots, 6$, where γ is a variable increasing from γ_L to γ_R. For convenience and simplicity, we assume $\gamma < -\frac{1}{\ln \rho_{max}}$ to ensure the curves will not intersect with each other.

Denoting the stationary contact discontinuity by $S_0(U_0, U)$, the states $U_* = (\rho_*, v_*, \gamma)$, $U^* = (\rho^*, v^*, \gamma)$, and $\hat{U} = (\hat{\rho}, \hat{v}, \gamma)$ have the following properties.

Lemma 2.3. *Given a left-hand state $U_0(\rho_0, v_0, \gamma_0)$ connected by $S_0(U_0, U)$, if $U_0 \in G_1 \cup G_6$, then ρ_* is selected; if $U_0 \in G_2 \cup G_5$, ρ^* is selected, and $\hat{\rho}$ is selected when $U_0 \in G_3 \cup G_4$.*

Proof. From (2.37) and (2.38), we can easily obtain $F(\rho_*) = 0$ and $F'(\rho_*) < 0$. It follows that

$$k(\gamma + 1)\rho_*^{\gamma} + k\gamma N\rho_*^{\gamma-1} < N, \tag{2.40}$$

where

$$N = (\rho_* + p_*)\frac{v_*^2}{1 - v_*^2} + p_*. \tag{2.41}$$

By substituting (2.41) into (2.40), we get that $v_*^2 > k\gamma\rho_*^{\gamma-1}$. Therefore, if $U_0 \in G_1 \cup G_6$, ρ_* is selected. The proof in the case of ρ^* is similar and the result of $\hat{\rho}$ is clearly valid. Thus, we prove the lemma. See Figure 2. □

Lemma 2.4. *The admissibility criterion is equivalent to the statement that stationary waves can only remain within the closure of the certain domain.*

Proof. Given the left-hand state $U_0(\rho_0, v_0, \gamma_0)$, we take the differential of (2.28) and then obtain

$$\begin{cases} (\rho + k\rho^{\gamma})\dfrac{2v}{(1 - v^2)^2}\mathrm{d}v + \left(\dfrac{v^2}{1 - v^2}\left(1 + k\gamma\rho^{\gamma-1}\right) + k\gamma\rho^{\gamma-1}\right)\mathrm{d}\rho \\ \qquad + \left(k\rho^{\gamma}\ln\rho\dfrac{v^2}{1 - v^2} + k\rho^{\gamma}\ln\rho\right)\mathrm{d}\gamma = 0, \\ (\rho + k\rho^{\gamma})\dfrac{1 + v^2}{(1 - v^2)^2}\mathrm{d}v + \dfrac{v}{1 - v^2}\left(1 + k\gamma\rho^{\gamma-1}\right)\mathrm{d}\rho + k\rho^{\gamma}\ln\rho\dfrac{v}{1 - v^2}\mathrm{d}\gamma = 0. \end{cases} \tag{2.42}$$

By Cramer's rule, we obtain

$$\begin{cases} \dfrac{\mathrm{d}v}{\mathrm{d}\gamma} = \dfrac{-kv\rho^{\gamma}\ln\rho\left(1 - v^2\right)}{(\rho + k\rho^{\gamma})(v^2 - k\gamma\rho^{\gamma-1})}, \\ \dfrac{\mathrm{d}\rho}{\mathrm{d}\gamma} = \dfrac{k\rho^{\gamma}\ln\rho}{v^2 - k\gamma\rho^{\gamma-1}}. \end{cases} \tag{2.43}$$

Since γ is increasing, $\mathrm{d}\gamma > 0$. So, we conclude that if $U_0 \in G_1 \cup G_6$, then the curve $S_0(U_0, U)$ increases with respect to v but decreases with respect to ρ. Similarly, when $U_0 \in G_2 \cup G_3 \cup G_4 \cup G_5$, the curve $S_0(U_0, U)$ decreases with respect to v but increases with respect to ρ. Thus, we prove the lemma. See Figure 2. □

Remark. By using Lemma 2.4, one can find that, $\lambda_1(U)$ has the same sign with $\lambda_1(U_0)$, and $\lambda_2(U)$ has the same sign with $\lambda_2(U_0)$. Thus, we claim that across the stationary wave, the number of characteristics impinging on it from the one side is equal to the number of characteristics leaving it from the other side.

We can compare the admissibility criterion with the Lax shock conditions (2.19). For the Lax shock conditions, the number of unknown variables on both sides together with shock speed ($2 \times 2 + 1 = 5$) equals the number of incoming characteristics (3) plus the number of relations across the shock wave (2). Similarly, for the stationary wave, the unknown variable is 4, which equals the number of incoming characteristics (2) plus the number of relations across the stationary wave (2). Thus, both the admissibility criterion and the Lax shock conditions are used to solve the unknown variables uniquely.

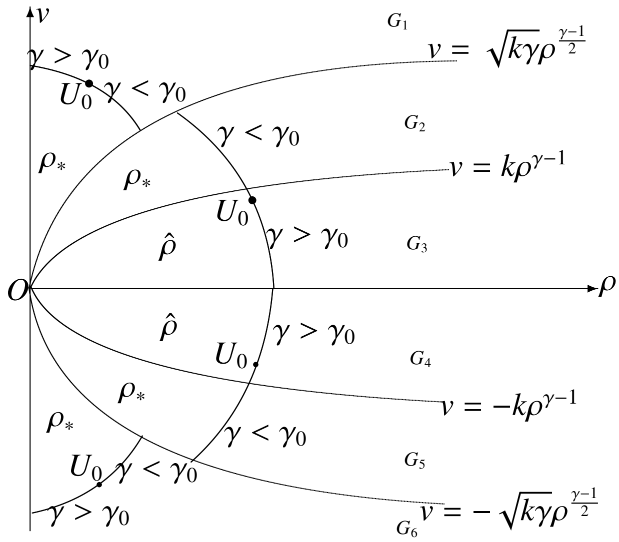

Figure 2. The curve of S_0 in the (ρ, v)-plane.

To obtain the Riemann solution, we need to determine the sign of the shock wave speed. In other words, we must determine the point at which the shock speed equals to zero.

When the shock speeds are zero, the Rankine-Hugoniot conditions are transformed into

$$\begin{cases} (\rho + p)\dfrac{v^2}{1 - v^2} + p = (\rho_0 + p_0)\dfrac{v_0^2}{1 - v_0^2} + p_0, \\ (\rho + p)\dfrac{v}{1 - v^2} = (\rho_0 + p_0)\dfrac{v_0}{1 - v_0^2}, \end{cases} \tag{2.44}$$

where γ is an invariant.

Therefore, the zero-speed shocks satisfy the following equation:

$$k\rho^{\gamma+1} + k\left((\rho_0 + p_0)\frac{v_0^2}{1 - v_0^2} + p_0\right)\rho^{\gamma} - \left((\rho_0 + p_0)\frac{v_0^2}{1 - v_0^2} + p_0\right)\rho + \frac{\rho_0^2 v_0^2 - p_0^2}{1 - v_0^2} = 0. \tag{2.45}$$

We can prove that $v^2 = p^2/\rho^2$ satisfies (2.45). In other words, the points at which the shock speed vanishes are in $\Sigma_2 \cup \Sigma_4$. If $U_0 \in G_1 \cup G_2$, there are two points $\rho_1 < \rho_2$ satisfying (2.45). Since

$\Sigma_2 : v = \frac{p}{\rho}$ is below Σ_1, the points on Σ_2 satisfy the condition $v^2 < p_\rho$. So, ρ_2 is on Σ_2, and $\rho_1 = \rho_0 \in G_1$. Precisely, we impose the following lemma.

Lemma 2.5. *(i) The 1-shock speed $\sigma_1(U_0, U)$ may change its sign along the backward 1-shock curve $S_1(U_0, U)(\rho > \rho_0)$. More precisely:*

(a) If $U_0 \in G_2 \cup G_3 \cup G_4 \cup G_5 \cup G_6$, then $\sigma_1(U_0, U)$ remains negative:

$$\sigma_1(U_0, U) < 0, \quad U \in S_1(U_0, U). \tag{2.46}$$

(b) If $U_0 \in G_1$, then there is a point $U = \tilde{U}_0 \in \Sigma_2$ that is on the shock curve $S_1(U_0, U)$ such that

$$\begin{cases} \sigma_1(U_0, \tilde{U}_0) = 0, \\ \sigma_1(U_0, U) > 0, \quad \rho \in (\rho_0, \tilde{\rho}_0), \\ \sigma_1(U_0, U) < 0, \quad \rho \in (\tilde{\rho}_0, +\infty). \end{cases} \tag{2.47}$$

(ii) The 2-shock speed $\sigma_2(U_0, U)$ may change its sign along the forward 2-shock curve $S_2(U_0, U)(\rho > \rho_0)$. More precisely:

(a) If $U_0 \in G_1 \cup G_2 \cup G_3 \cup G_4 \cup G_5$, then $\sigma_2(U_0, U)$ remains positive:

$$\sigma_2(U_0, U) > 0, \quad U \in S_2(U_0, U). \tag{2.48}$$

(b) If $U_0 \in G_6$, then there is a point $U = \tilde{U}_0 \in \Sigma_4$ that is on the shock curve $S_2(U, U_0)$ such that

$$\begin{cases} \sigma_2(U_0, \tilde{U}_0) = 0, \\ \sigma_2(U_0, U) < 0, \quad \rho \in (\rho_0, \tilde{\rho}_0), \\ \sigma_2(U_0, U) > 0, \quad \rho \in (\tilde{\rho}_0, +\infty). \end{cases} \tag{2.49}$$

3. The Riemann problem

In this section, we are mainly interested in the case that γ is piecewise constant,

$$\gamma(x) = \begin{cases} \gamma_L, & x < 0, \\ \gamma_R, & x > 0, \end{cases} \tag{3.1}$$

where γ_L, γ_R are two distinct constants. The Riemann problem associated with (2.1) is the initial-value problem corresponding to

$$(\rho, v, \gamma) = \begin{cases} (\rho_L, v_L, \gamma_L), & x < 0, \\ (\rho_R, v_R, \gamma_R), & x > 0. \end{cases} \tag{3.2}$$

To project all the wave curves on the (ρ, v)-plane, we use the following notations:

(i)$W_k(U_i, U_j)$ $\left(S_k(U_i, U_j), R_k(U_i, U_j)\right)$ denotes the kth-wave (kth-shock, kth-rarefaction wave) from the left-hand state U_i to the right-hand state U_j.

(ii)$W_m(U_i, U_j) \to W_n(U_j, U_k)$ indicates that there exists an mth-wave connecting the left-hand state U_i to the right-hand state U_j, followed by an nth-wave connecting the left-hand state U_j to the right-hand state U_k.

In [14], the Riemann problem for a constant γ has been solved. The shock waves and the rarefaction waves separate the whole (v, ρ) plane into four regions, and there are in total four cases for the Riemann problem, namely $\overleftrightarrow{RR}$, $\overleftrightarrow{RS}$, $\overleftrightarrow{SR}$, $\overleftrightarrow{SS}$. In the current system where γ changes, a degenerate characteristic field is introduced and the system is not strictly hyperbolic. The coalescence of waves and resonance phenomenon will appear, thus the Riemann problem is more complicated. We still use the characteristic analysis method in the phase plane to classify the initial data and construct the solution, which may include the following 9 cases.

3.1. The Riemann solutions for $U_L \in G_1$

Case 1:

This construction holds for $U_R \in G_1 \cup \Sigma_1$ and some part of G_2. See Figure 3. First, we define $U_1 \in G_1$, which is a jump from U_L by a stationary contact from $\gamma = \gamma_L$ to $\gamma = \gamma_R$. If $W_1(U_1) \cap W_2(U_R) \neq \phi$, there exists a solution defined as follows. Denote $\{U_2\} = W_1(U_1) \cap W_2(U_R)$. Then, the Riemann solution is

$$S_0(U_L, U_1) \to W_1(U_1, U_2) \to W_2(U_2, U_R). \tag{3.3}$$

The construction holds for $\sigma_1(U_1, U_2) \geq 0$.

If $W_1(U_1) \cap W_2(U_R) = \phi$, there exists a vacuum. Denote $\{X\} = W_1(U_1) \cap \{\rho = 0\}$ and $\{Y\} = W_2(U_R) \cap \{\rho = 0\}$, the Riemann solution is

$$S_0(U_L, U_1) \to W_1(U_1, X) \to \text{Vacuum}(X, Y) \to W_2(Y, U_R). \tag{3.4}$$

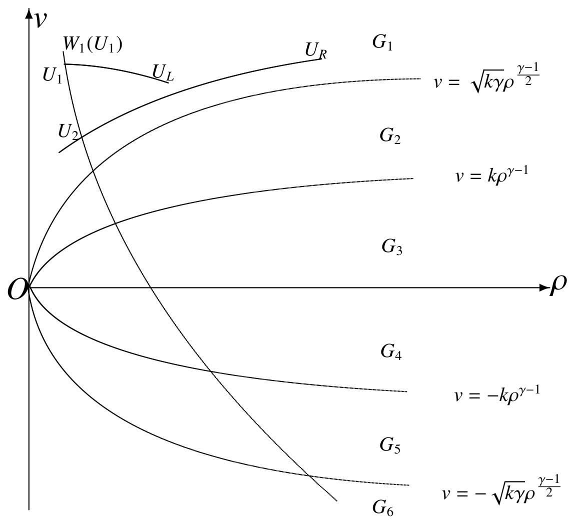

Figure 3. $U_R \in G_1 \cup \Sigma_1$ and some part of G_2.

Case 2:

This construction holds for $U_R \in G_3 \cup G_4 \cup \Sigma_2 \cup \Sigma_3$ and some part of $G_1 \cup G_2 \cup G_5 \cup G_6 \cup \Sigma_1 \cup \Sigma_4$. See Figure 4. We define the point $\tilde{U}_L \in W_1(U_L) \cap \Sigma_3$ at which the shock speed vanishes ($\sigma_1(U_L, \tilde{U}_L) = 0$). From any point $U = (\rho, v) \in W_1(U_L)$, $\rho \geq \tilde{\rho}_L$, we define the state $\bar{U}$ which is a jump from U by a stationary wave with $\gamma = \gamma_L$ to $\gamma = \gamma_R$. These states can form a curve denoted by $W_\gamma(U_L)$. To be precise, set

$$W_\gamma(U_L) := \left\{\bar{U} : \exists S_0\left(U, \bar{U}\right) \text{ from } \gamma_L \text{ to } \gamma_R, U = (\rho, v) \in W_1\left(U_L\right), \rho \geq \tilde{\rho}_L\right\}.$$

Whenever $W_2(U_R) \cap W_\gamma(U_L) \neq \phi$, there will be a solution. Denote $\{U_4\} = W_2(U_R) \cap W_\gamma(U_L)$, and U_3 is the point in $W_1(U_L)$ which corresponds to the stationary wave $S_0(U_3, U_4)$. Then, the Riemann solution is

$$S_1(U_L, U_3) \to S_0(U_3, U_4) \to W_2(U_4, U_R). \tag{3.5}$$

The construction holds for $\sigma_2(U_4, U_R) \geq 0$.

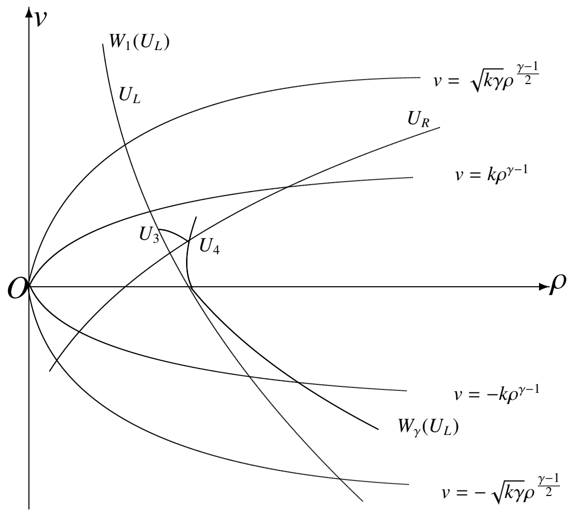

Figure 4. $U_R \in G_3 \cup G_4 \cup \Sigma_2 \cup \Sigma_3\ (G_1 \cup G_2 \cup G_5 \cup G_6 \cup \Sigma_1 \cup \Sigma_4)$.

Case 3:

This construction shows a connection between Case 1 and Case 2. See Figure 5. We consider a solution containing three waves with the same zero speed. First, U_L jumps to A by a stationary wave $S_0(U_L, A := U_L(\gamma))$ with an intermediate value $\gamma \in [\gamma_L, \gamma_R]$. Then, A jumps to $B := \tilde{A}$ by $S_1(A, B)$ with $\sigma_1(A, B) = 0$. Next, B jumps to the state $C := U(\gamma)$ by another stationary wave to shift the level γ to γ_R. Denote

$$L := \{U(\gamma) \mid \gamma \in [\gamma_L, \gamma_R]\}.$$

Whenever $W_2(U_R) \cap L \neq \phi$, the solution contains three discontinuities with the same zero speed as follows:

$$S_0(U_L, A) \to S_1(A, B) \to S_0(B, C) \to W_2(C, U_R). \tag{3.6}$$

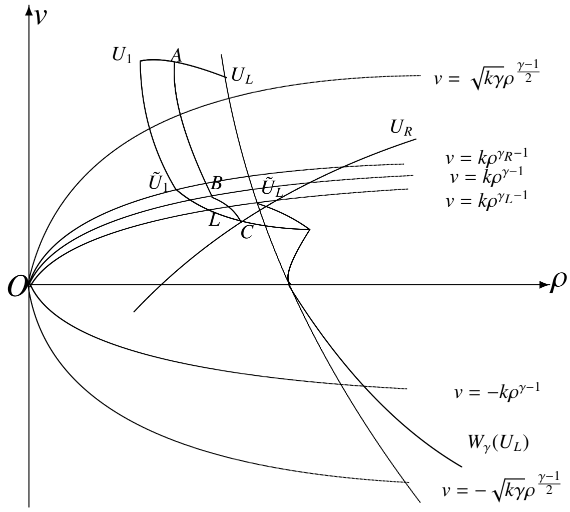

Figure 5. The construction of Case 3.

Case 4:

This construction holds for arbitrary U_L in the whole domain. See Figure 6. For $U_R \in G_6$, we define the point $U_8 \in G_6$ as the state jumping to U_R with a stationary wave. Then, denote $\{U_7\} = W_1(U_L) \cap W_2(U_8)$. If $U_7 \in G_5 \cup G_6$, there is a Riemann solution of the form

$$S_1(U_L, U_7) \to W_2(U_7, U_8) \to S_0(U_8, U_R). \tag{3.7}$$

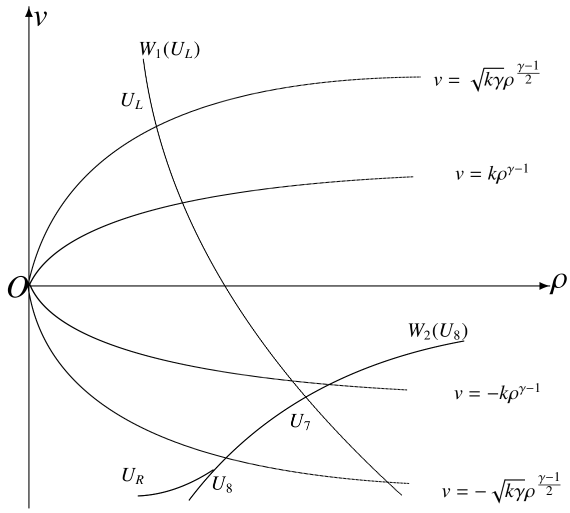

Figure 6. The construction for arbitrary U_L in the whole domain.

Case 5:

This construction holds for U_R in some part of G_6. See Figure 7. There are solutions containing three waves with the same zero speed. First, U_L jumps to the state E by 1-shock $S_1(U_L, E)$ with negative speed. Then, E jumps to F by a stationary wave $S_0(E, F)$ with an intermediate value $\gamma \in [\gamma_L, \gamma_R]$, where F is followed by a 2-shock with $\sigma_2(F, P) = 0$ to the state $P \in G_6$. Finally, P jumps to U_R by another stationary wave with the level γ to γ_R. The solution contains three discontinuities with the same zero speed of the form

$$S_1(U_L, E) \to S_0(E, F) \to S_2(F, P) \to S_0(P, U_R). \tag{3.8}$$

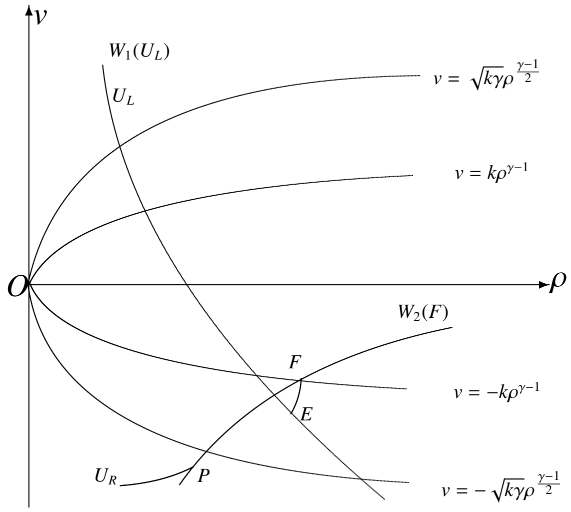

Figure 7. U_R in some part of G_6.

Existence of the Riemann problem. When $\gamma = \gamma_L$, the curve L intersects $W_1(U_1)$ at the point $\tilde{U}_L$. When $\gamma = \gamma_R$, the curve L meets $W_\gamma(U_L)$. These paths form a locally Lipschitz continuous curve in the (ρ, v)-plane. In Cases 1–3, the Riemann problem admits a solution if $W_2(U_R)$ intersects this curve. In Case 4, the solution exists if $U_7 \in G_5 \cup G_6$. A sufficient condition for the existence of a Riemann solution is given as follows:

(1) $W_2(U_R)$ intersects the curve $W_1(U_R) \cup L \cup W_\gamma(U_\gamma)$.
(2) $U_R \in G_6$ for $U_7 \in G_5 \cup G_6$.

Uniqueness of the Riemann problem. If the right-hand state U_R is chosen such that Case 1 makes sense, then a unique Riemann solution is obtained. Geometrically, $W_2(U_R)$ does not intersect the curve $W_\gamma(U_\gamma) \cup L$. Since the mapping $\gamma \mapsto U(\gamma)$, $\gamma \in [\gamma_L, \gamma_R]$ is locally Lipschitz continuous, and the curve L is close to $\tilde{U}_L$ when $|\gamma_R - \gamma_L|$ is sufficiently small. For large $|\gamma_R - \gamma_L|$, an alternative a priori estimate is that $W_2(U_R)$ lies entirely in the region G_1. This occurs when the velocity v is non-negative at the intersection of this curve with the axis $\rho = 0$. Setting $\rho = 0$ in (2.15), we have

$$\frac{1}{2}\ln\left(\frac{1+v_R}{1-v_R}\right) > \int_0^{\rho_R} \frac{\sqrt{p'(z)}}{z+p(z)} dz. \tag{3.9}$$

Thus, we have the following theorem.

Theorem 3.1. *For the given $U_L \in G_1$, if $W_2(U_R)$ intersects the curve $W_1(U_R) \cup L \cup W_\gamma(U_\gamma)$, or $U_R \in G_6$ and $U_7 \in G_5 \cup G_6$, then the Riemann problem for* (2.1) *admits a solution. In particular, if* (3.9) *holds or $|\gamma_R - \gamma_L|$ is sufficiently small, there exists a unique Riemann solution.*

3.2. The Riemann solutions for $U_L \in G_2 \cup G_3 \cup G_4 \cup G_5 \cup G_6$

Case 6:

This construction holds for $U_R \in G_1 \cup \Sigma_1$ and some part of G_2. See Figure 8. First, we define $\{D\} = W_1(U_L) \cap \{(\rho, v)|v = \sqrt{k\gamma_L}\rho^{\frac{\gamma_L-1}{2}}\}$. The solution begins with a 1-rarefaction wave $R_1(U_L, D)$ and jumps from D to U_1 by a stationary wave using ρ_* at D. Denote $\{U_2\} = W_1(U_1) \cap W_2(U_R)$. Then, the solution can jump from U_1 to U_2 by $W_1(U_1, U_2)$ and is continued by $W_2(U_2, U_R)$ from U_2 to U_R. Thus, whenever $W_1(U_1) \cap W_2(U_R) \neq \phi$, there exists a solution defined as follows:

$$R_1(U_L, D) \to S_0(D, U_1) \to W_1(U_1, U_2) \to W_2(U_2, U_R). \tag{3.10}$$

The construction holds for $\sigma_1(U_1, U_2) \geq 0$.

If $W_1(U_1) \cap W_2(U_R) = \phi$, there exists a vacuum. Denote $\{X\} = W_1(U_1) \cap \{\rho = 0\}$ and $\{Y\} = W_2(U_R) \cap \{\rho = 0\}$, the Riemann solution is

$$R_1(U_L, D) \to S_0(D, U_1) \to W_1(U_1, X) \to \text{Vacuum}(X, Y) \to W_2(Y, U_R). \tag{3.11}$$

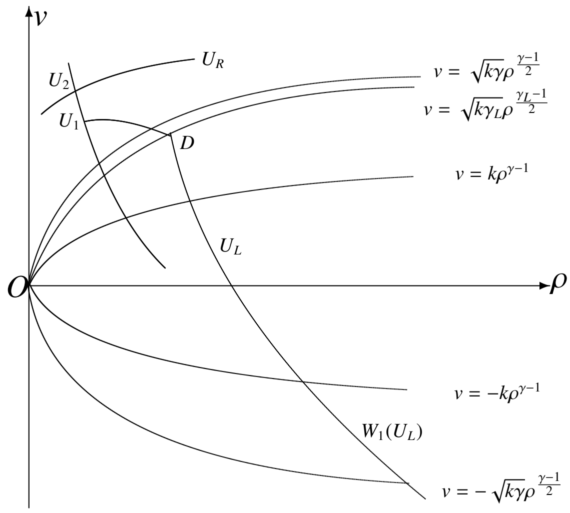

Figure 8. $U_R \in G_1 \cup \Sigma_1$ and some part of G_2.

Case 7:

This construction holds for $U_R \in G_3 \cup G_4 \cup \Sigma_2 \cup \Sigma_3$ and some part of $G_1 \cup G_2 \cup G_5 \cup G_6 \cup \Sigma_1 \cup \Sigma_4$. See Figure 9. We denote the point K which is jumped by a stationary wave from D using ρ^*. Similar to Case 2, we can define the curve

$$W_\gamma(U_L) := \left\{\bar{U} : \exists S_0\left(U, \bar{U}\right) \text{ from } \gamma_L \text{ to } \gamma_R, U = (\rho, v) \in W_1(U_L), \rho \geq \tilde{\rho}_D\right\}.$$

Whenever $W_2(U_R) \cap W_\gamma(U_L) \neq \phi$, there will be a solution. Denote $\{U_4\} = W_2(U_R) \cap W_\gamma(U_L)$, and U_3 is the point in $W_1(U_L)$ which corresponds to the stationary wave $S_0(U_3, U_4)$. Then, the Riemann solution is

$$W_1(U_L, U_3) \to S_0(U_3, U_4) \to W_2(U_4, U_R). \tag{3.12}$$

The construction holds for $\sigma_2(U_4, U_R) \geq 0$.

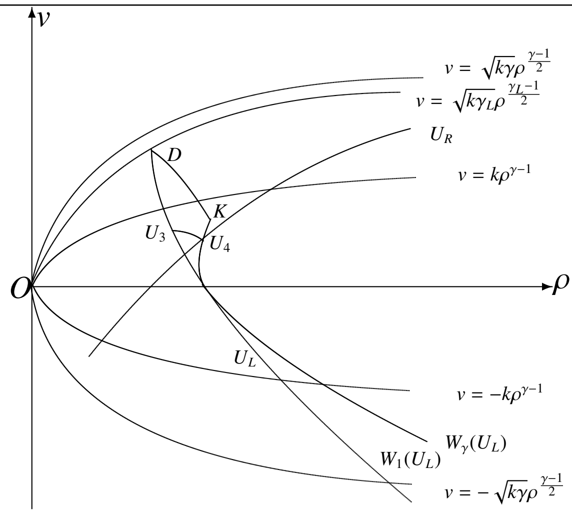

Figure 9. $U_R \in G_3 \cup G_4 \cup \Sigma_2 \cup \Sigma_3$ $(G_1 \cup G_2 \cup G_5 \cup G_6 \cup \Sigma_1 \cup \Sigma_4)$.

Case 8:

This construction shows a connection between Case 6 and Case 7. See Figure 10. We also consider a solution containing three waves with the same zero speed. First, U_L jumps to D by a 1-rarefaction wave $R_1(U_L, D)$. Then, D jumps to some state $E := U_L(\gamma) \in G_1$ with a shift in γ from γ_L to an intermediate value $\gamma \in [\gamma_L, \gamma_R]$, then followed by a 1-shock $S_1(E, F)$ with zero speed, where $F := \tilde{E} \in G_3$. Next, F jumps to the state $H := U(\gamma)$ by another stationary wave to shift the level γ to γ_R. As γ varies continuously on $[\gamma_L, \gamma_R]$, $U(\gamma)$ can form a curve Λ with $U(\gamma_R) = J := \tilde{U}_1$ and $U(\gamma_L) = K$. Set

$$\Lambda := \{U(\gamma) \mid \gamma \in [\gamma_L, \gamma_R]\}.$$

If $W_2(U_R) \cap \Lambda \neq \phi$, then the Riemann problem can be

$$R_1(U_L, D) \to S_0(D, E) \to S_1(E, F) \to S_0(F, H) \to W_2(H, U_R). \tag{3.13}$$

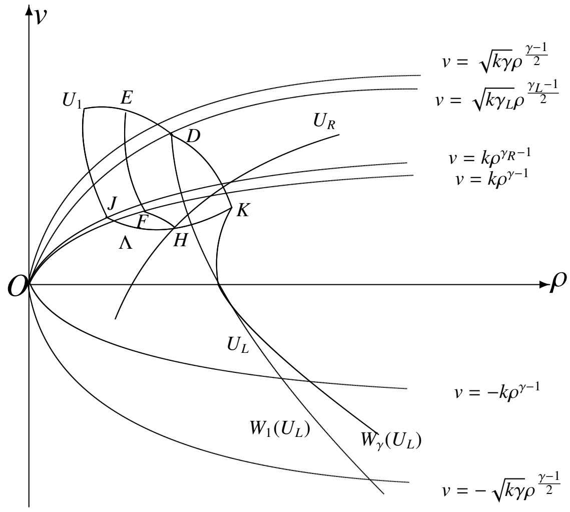

Figure 10. The construction of Case 8.

The curve Λ connects $W_1(U_1)$ in Case 6 and $W_\gamma(U_1)$ in Case 7, so the existence and uniqueness of the Riemann problem can be argued similarly as in the case $U_L \in G_1$.

Case 9:

This construction holds for $U_L \in G_6$ and some part of $G_4 \cup G_5 \cup \Sigma_4 \cup \Sigma_5$. See Figure 11. For each point $U_2 \in \{(\rho, v) | v = -\sqrt{k\gamma_L}\rho^{\frac{\gamma_L-1}{2}}\}$, we define a curve that is formed by taking the resulting states of the stationary wave from U_2 using ρ^*. Then, this curve intersects $W_2(U_R)$ at U_3. Whenever $W_1(U_L) \cap W_2(U_2) \neq \phi$, there exists a solution defined as follows. Denote $\{U_1\} = W_1(U_L) \cap W_2(U_2)$. Then the Riemann solution is

$$W_1(U_L, U_1) \rightarrow W_2(U_1, U_2) \rightarrow S_0(U_2, U_3) \rightarrow W_2(U_3, U_R). \tag{3.14}$$

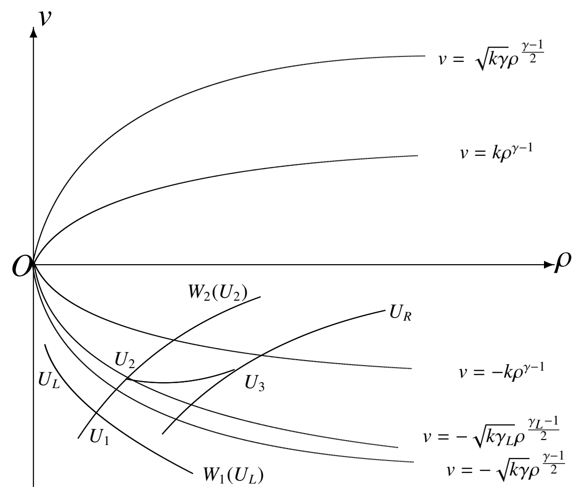

Figure 11. $U_L \in G_6$ and some part of $G_4 \cup G_5 \cup \Sigma_4 \cup \Sigma_5$.

Note that in Case 7, if $|\gamma_R - \gamma_L|$ is sufficiently small, the curve Λ is close to the point D. Therefore, if $|U_R - U_L| + |\gamma_R - \gamma_L|$ is sufficiently small, $W_2(U_R)$ does not intersect $W_1(U_1) \cup \Lambda$, so the Riemann problem for (2.1) has a unique solution. In Case 4, if $|U_R - U_L| + |\gamma_R - \gamma_L|$ is sufficiently small, the Riemann solution is also unique. Thus, we have the following theorem.

Theorem 3.2. *For the given $U_L \in G_2 \cup G_3 \cup G_4 \cup G_5 \cup G_6 \cup \Sigma_1 \cup \Sigma_2 \cup \Sigma_3 \cup \Sigma_4 \cup \Sigma_5$, if the curve $W_2(U_R)$ intersects the curve $W_1(U_1) \cup \Lambda \cup W_\gamma(U_L)$, or $U_L \in G_6$ and* (3.7) *or* (3.12) *is constructed, then the Riemann problem for* (2.1) *admits a solution. In particular, if $|U_R - U_L| + |\gamma_R - \gamma_L|$ is sufficiently small, there exists a unique Riemann solution.*

4. The interactions of rarefaction wave or shock wave with the stationary wave

To study the interactions of rarefaction waves or shock waves with stationary waves, we consider the initial value problem of (2.1) with the initial data

$$(\rho, v, \gamma)\,|_{t=0} = \begin{cases} U_L = (\rho_L, v_L, \gamma_L), & x < x_1, \\ U_m = (\rho_m, v_m, \gamma_L), & x_1 < x < x_2, \\ U_R = (\rho_R, v_R, \gamma_R), & x > x_2. \end{cases} \tag{4.1}$$

4.1. The interaction of rarefaction wave with stationary wave

The initial conditions in this case are

$$U_m \in R_2(U_L, U), \quad U_R \in S_0(U_m, U).$$

We have

$$\begin{cases} U_0(\rho_0, v_0, \gamma_L) \in R_2(U, U_m) : \dfrac{1}{2}\ln\left(\dfrac{1+v_0}{1-v_0}\right) - \dfrac{1}{2}\ln\left(\dfrac{1+v_m}{1-v_m}\right) = \displaystyle\int_{\rho_m}^{\rho_0} \dfrac{\sqrt{p'(z)}}{z+p(z)}\mathrm{d}z, \\ U_1(\rho, v, \gamma_R) \in S_0(U_0, U) : \begin{cases} (\rho+p)\dfrac{v}{1-v^2} = (\rho_0+p_0)\dfrac{v_0}{1-v_0^2}, \\ (\rho+p)\dfrac{v^2}{1-v^2} + p = (\rho_0+p_0)\dfrac{v_0^2}{1-v_0^2} + p_0. \end{cases} \end{cases} \tag{4.2}$$

We define the following curves Γ_1, Γ_*, Γ_+, and Γ^* in the (ρ, v)-plane. Γ_* and Γ^* denote the states followed by $S_0(U_0, U)$ using ρ_* and ρ^* respectively from $U_0 \in \Gamma_+$. Γ_1 is the rarefaction curve $R_2((0,0), U)$ between Γ_* and Γ^*, which will be proved. We have the following lemma.

Lemma 4.1. Γ_1 *is between* Γ_* *and* Γ_+ *in the* (ρ, v)*-plane. See Figure 12.*

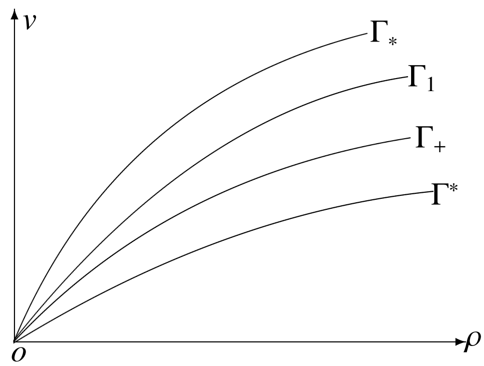

Figure 12. The relative positions of Γ_1,Γ_* and Γ^*.

Proof. Let us first prove Γ_1 is above Γ_+. For the curve Γ_+, we can parameterize it as $v_+ = v_+(\rho)$, and obtain that

$$s_+ = \frac{\mathrm{d}v_+}{\mathrm{d}\rho} = \frac{\gamma-1}{2}\sqrt{k\gamma}\rho^{\frac{\gamma-3}{2}}.$$

Similarly, for the curve Γ_1, we parameterize it as $v_1 = v_1(\rho)$, and have

$$s_1 = \frac{\mathrm{d}v_1}{\mathrm{d}\rho} = \frac{\sqrt{p'(\rho)}(1-v_1^2)}{\rho+p} = \frac{1-v_1^2}{1+k\rho^{\gamma-1}}\sqrt{k\gamma}\rho^{\frac{\gamma-3}{2}}.$$

Since $p'(\rho) = k\gamma\rho^{\gamma-1} < 1$, $k\rho^{\gamma-1} < \frac{1}{\gamma}$ and then $s_1 > (1-v_1^2)\frac{\gamma}{1+\gamma}\sqrt{k\gamma}\rho^{\frac{\gamma-3}{2}}$. In addition, we compare s_+ and s_1, and know that

$$\frac{\gamma-1}{2}\cdot\frac{1+\gamma}{\gamma} = \frac{\gamma^2-1}{2\gamma} \in (0, \frac{8}{15})$$

is an increasing function of γ. Therefore, when v_1^2 is less than $\frac{2\gamma+1-\gamma^2}{2\gamma}$, Γ_1 is above Γ_+.

Next, we turn to prove Γ_1 is below Γ_*. Letting $U_0 \in \Gamma_+$, we have

$$v_0 = \sqrt{p'(\rho_0)}, \quad \frac{\mathrm{d}v_0}{\mathrm{d}\rho_0} = \frac{p''(\rho_0)}{2\sqrt{p'(\rho_0)}} = \frac{p''(\rho_0)}{2v_0}.$$

From 4.2, we differentiate the three equations, respectively, and have

$$\frac{(1+\sqrt{p'(\rho_0)})\frac{v_0}{1-v_0} + (\rho_0+p_0)\frac{1+v_0^2}{(1-v_0^2)^2}\frac{p''(\rho_0)}{2v_0}}{\frac{v_0^2+p'(\rho_0)}{1-v_0^2} + (\rho_0+p_0)\frac{2v_0}{(1-v_0^2)^2}\frac{p''(\rho_0)}{2v_0}} = \frac{(1+\sqrt{p'(\rho)})\frac{v}{1-v} + (\rho+p)\frac{1+v^2}{(1-v^2)^2}\frac{\mathrm{d}v}{\mathrm{d}\rho}}{\frac{v^2+p'(\rho)}{1-v^2} + (\rho+p)\frac{2v}{(1-v^2)^2}\frac{\mathrm{d}v}{\mathrm{d}\rho}}.$$

Since $v_0 = \sqrt{p'(\rho_0)}$, so we obtain

$$\frac{(1+v_0^2)\frac{v_0}{1-v_0} + (\rho_0+p_0)\frac{1+v_0^2}{(1-v_0^2)^2}\frac{p''(\rho_0)}{2v_0}}{\frac{2v_0^2}{1-v_0^2} + (\rho_0+p_0)\frac{2v_0}{(1-v_0^2)^2}\frac{p''(\rho_0)}{2v_0}} = \frac{(1+p'(\rho))\frac{v}{1-v} + (\rho+p)\frac{1+v^2}{(1-v^2)^2}\frac{\mathrm{d}v}{\mathrm{d}\rho}}{\frac{v^2+p'(\rho)}{1-v^2} + (\rho+p)\frac{2v}{(1-v^2)^2}\frac{\mathrm{d}v}{\mathrm{d}\rho}},$$

which yields

$$\begin{aligned}&(1-v^2)\left[(v^2+p'(\rho))(1+v_0^2) - 2vv_0(1+p'(\rho))\right]\left[2v_0^2(1-v_0^2) + (\rho_0+p_0)p''(\rho_0)\right]\\ &= (v-v_0)(vv_0-1)(\rho+p)\left[4v_0^2(1-v_0^2) + 2(\rho_0+p_0)p''(\rho_0)\right]\frac{\mathrm{d}v}{\mathrm{d}\rho}.\end{aligned}$$

Thus, we get

$$s_* = \frac{\mathrm{d}v}{\mathrm{d}\rho} = \frac{(1-v^2)\left[p'(\rho)(1+v_0^2-2vv_0) + v^2 + v^2v_0^2 - 2vv_0\right]}{2(\rho+p)(v-v_0)(vv_0-1)}.$$

So, we get

$$s_* - s_1 = \frac{(1-v^2)\left[p'(\rho)(1+v_0^2-2vv_0) + v^2 + v^2v_0^2 - 2vv_0\right]}{2(\rho+p)(v-v_0)(vv_0-1)} - \frac{\sqrt{p'(\rho)}(1-v_1^2)}{\rho+p}.$$

Consider the intersection of two curves, that is, $v_1 = v$. We have

$$\begin{aligned}&\frac{(1-v^2)\left[p'(\rho)(1+v_0^2-2vv_0) + v^2 + v^2v_0^2 - 2vv_0\right]}{2(\rho+p)(v-v_0)(vv_0-1)} - \frac{\sqrt{p'(\rho)}(1-v^2)}{\rho+p}\\ &= \frac{(1-v^2)\left[p'(\rho)(1+v_0^2-2vv_0) + v^2 + v^2v_0^2 - 2vv_0 + 2(v-v_0)(1-vv_0)\sqrt{p'(\rho)}\right]}{2(\rho+p)(v-v_0)(vv_0-1)}.\\ &= \frac{(1-v^2)(v+\sqrt{p'(\rho)})\left[\sqrt{p'(\rho)}(1+v_0^2-2vv_0) + v + vv_0^2 - 2v_0\right]}{2(\rho+p)(v-v_0)(vv_0-1)}.\end{aligned}$$

For convenience and simplicity, we consider the case

$$\frac{v+\sqrt{p'(\rho)}}{v\sqrt{p'(\rho)}+1} < \frac{v_0+\sqrt{p'(\rho_0)}}{v_0\sqrt{p'(\rho_0)}+1}. \tag{4.3}$$

The other case can be discussed similarly. Then, from $v_0 = \sqrt{p'(\rho_0)}$, we can obtain

$$\sqrt{p'(\rho)}(1 + v_0^2 - 2vv_0) + v + vv_0^2 - 2v_0 < 0.$$

Hence, initially, Γ_1 is below Γ_* near the intersection point $(0, 0)$, and we know $v_1 > v$ holds near $(0, 0)$. By the method of iteration, we get that $s_* - s_1 > 0$ if $v_1 > v$. So, Γ_1 is below Γ_*. We complete the proof of Lemma 4.1. □

Lemma 4.2. *The curve* Γ_1 *has the following properties:*

(1) If U_m *is above* Γ_1*, then* $R_2(U_0, U_m)$ *has a unique intersection* $\bar{U} = (0, \bar{v})$ *with the* v*-axis and* $S_0(U_0, U_1) \cap R_2(U_0, U_m) = \{\bar{U}\}$.

(2) If U_m *is below* Γ_1*, then* $R_2(U_0, U_m)$ *has a unique intersection* $\bar{U} = (\bar{\rho}, 0)$ *with the* ρ*-axis and* $S_0(U_0, U_1) \cap R_2(U_0, U_m) = \{\bar{U}\}$.

Lemma 4.3. *The relative positions of the curves* $S_0(U_0, U_1)$ *and* $R_2(U, U_R)$ *are shown as follows:*

(1) If U_R *is above* Γ_**,* $R_2(U, U_R)$ *is above* $S_0(U_0, U_1)$*. See Figure 13 (left).*

(2) If U_R *is between* Γ_* *and* Γ^**, there are no stationary waves.*

(3) If U_R *is below* Γ_**,* $R_2(U, U_R)$ *is below* $S_0(U_0, U_1)$*. See Figure 13 (left).*

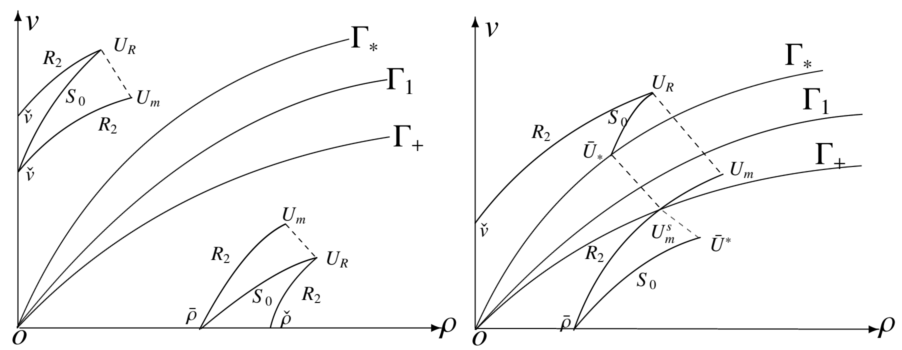

Figure 13. The relative positions of the curves $S_0(U_0, U_1)$ and $R_2(U, U_R)$.

Proof. For $U_0(\rho_0, v_0, \gamma_L) \in R_2(U, U_m)$, we have

$$\frac{\mathrm{d}v_0}{\mathrm{d}\rho_0} = \frac{\sqrt{p'(\rho_0)}(1 - v_0^2)}{\rho_0 + p_0}.$$

From 4.2, we get

$$\begin{cases} (1 + p'(\rho_0))\dfrac{v_0}{1 - v_0^2}\mathrm{d}\rho_0 + (\rho_0 + p_0)\dfrac{1 + v_0^2}{(1 - v_0^2)^2}\mathrm{d}v_0 = (1 + p'(\rho))\dfrac{v}{1 - v^2}\mathrm{d}\rho + (\rho + p)\dfrac{1 + v^2}{(1 - v^2)^2}\mathrm{d}v, \\ \dfrac{v_0^2 + p'(\rho_0)}{1 - v_0^2}\mathrm{d}\rho_0 + (\rho_0 + p_0)\dfrac{2v_0}{(1 - v_0^2)^2}\mathrm{d}v_0 = \dfrac{v^2 + p'(\rho)}{1 - v^2}\mathrm{d}\rho + (\rho + p)\dfrac{2v}{(1 - v^2)^2}\mathrm{d}v. \end{cases}$$

After simplifying it, we get

$$\frac{v_0\sqrt{p'(\rho_0)} + 1}{v_0 + \sqrt{p'(\rho_0)}} = \frac{(1 + p'(\rho))v(1 - v^2) + (\rho + p)(1 + v^2)\frac{\mathrm{d}v}{\mathrm{d}\rho}}{(v^2 + p'(\rho))(1 - v^2) + 2v(\rho + p)\frac{\mathrm{d}v}{\mathrm{d}\rho}}.$$

Then

$$s_0 = \frac{dv}{d\rho} = \frac{(1-v^2)\left[(v^2+p'(\rho))(v_0\sqrt{p'(\rho_0)}+1)-(v_0+\sqrt{p'(\rho_0)})(1+p'(\rho))v\right]}{(\rho+p)\left[(v_0+\sqrt{p'(\rho_0)})(1+v^2)-2v(v_0\sqrt{p'(\rho_0)}+1)\right]}.$$

For the curve $R_2(U, U_R)$, we have

$$s_2 = \frac{dv_2}{d\rho} = \frac{\sqrt{p'(\rho)}(1-v_2^2)}{\rho+p}.$$

We consider the intersection U_R, that is, $v_2 = v$,

$$\begin{aligned} s_0 - s_2 =& \frac{(1-v^2)(v+\sqrt{p'(\rho)})}{\rho+p}\cdot \\ & \frac{(v+\sqrt{p'(\rho)})(v_0\sqrt{p'(\rho_0)}+1)-(v_0+\sqrt{p'(\rho_0)})(v\sqrt{p'(\rho)}+1)}{(v_0\sqrt{p'(\rho_0)}+v_0)(1+v^2)-2v(v_0\sqrt{p'(\rho_0)}+1)}. \end{aligned}$$

We know that if $v > \sqrt{p'(\rho)}$, then $v > v_0 > \sqrt{p'(\rho_0)}$. Thus, we can obtain

$$\begin{aligned} &(v_0\sqrt{p'(\rho_0)}+v_0)(1+v^2)-2v(v_0\sqrt{p'(\rho_0)}+1) \\ &= \sqrt{p'(\rho_0)}(1+v^2-2vv_0)+v_0+v_0v^2-2v \\ &< v_0(1+v^2-2vv_0)+v_0+v_0v-2v \\ &= 2(v-v_0)(v_0v-1) < 0. \end{aligned}$$

Analogously, we conclude that if $v < \sqrt{p'(\rho)}$, then $v < v_0 < \sqrt{p'(\rho_0)}$. Then, we get

$$\begin{aligned} &(v_0\sqrt{p'(\rho_0)}+v_0)(1+v^2)-2v(v_0\sqrt{p'(\rho_0)}+1) \\ &= \sqrt{p'(\rho_0)}(1+v^2-2vv_0)+v_0+v_0v^2-2v \\ &> v_0(1+v^2-2vv_0)+v_0+v_0v-2v \\ &= 2(v-v_0)(v_0v-1) > 0. \end{aligned}$$

In addition,

$$\begin{aligned} &(v+\sqrt{p'(\rho)})(v_0\sqrt{p'(\rho_0)}+1)-(v_0+\sqrt{p'(\rho_0)})(v\sqrt{p'(\rho)}+1) \\ &= (v\sqrt{p'(\rho)}+1)(v_0\sqrt{p'(\rho_0)}+1)\left(\frac{v+\sqrt{p'(\rho)}}{v\sqrt{p'(\rho)}+1}-\frac{v_0+\sqrt{p'(\rho_0)}}{v\sqrt{p'(\rho_0)}+1}\right) < 0. \end{aligned}$$

By the method of iteration, we can obtain that $s_0 - s_2 > 0, v_2 > v$ when U_R is above Γ_*, and $s_0 - s_2 < 0, v_2 < v$ when U_R is below Γ^*. □

Γ_1 and Γ_+ divide the (ρ, v)-plane into four subdomains, denoted by V_1, V_2, V_3, and V_4. In combination with the above discussion, we have:

(1) $U_R \in V_1$, the location of U_m has two subcases:

   (a) U_m is above Γ_1. $S_0(U_0, U_1)$ intersects the v-axis at the point $(0, \bar{v})$. Since $s_0 - s_2 > 0$, $S_0(U_0, U_1)$ is below $R_2(U, U_R)$. See Figure 13 (left).

(b) U_m is below Γ_1. Denote $\{U_m^s\} = R_2(U, U_m) \cap \Gamma_+$, $\bar{U}_*$ and $\bar{U}^*$ is jumped by $S_0(U_m, U)$ from U_m respectively using ρ_* and ρ^*. And, $S_0(U_0, U_1)$ is between $R_2(U, U_R)$ and Γ_* since $s_0 - s_2 > 0$. See Figure 13 (right).

(2) $U_R \in V_2 \cup V_3$. No solutions.

(3) $U_R \in V_4$, $U_m \in V_4$. Since $s_0 - s_2 < 0$ when $0 \leq v_1 \leq v_R$, then $S_0(U_0, U_1)$ is above $R_2(U, U_R)$. See Figure 13 (left).

Next, we will discuss their interaction case by case.

Case 1:

$U_R \in V_1$, U_m is above Γ_1. See Figure 14 (left).

We draw $R_2(U, U_R)$, $R_2(U, U_m)$, $S_0(U_0, U_1)$, and $R_1(\check{U})$ passing through $\check{U} = (0, \check{v})$. Denote $\{Q_*\} = R_1(\check{U}) \cap S_0(U_0, U_1)$, which is obtained from $Q \in R_2(U, U_m)$ by the stationary wave.

Case 1.1:

U_L is between Q and U_R. See Figure 14. Consider the initial boundary value problem (2.1) with

$$(\rho, v) = \begin{cases} (\rho_R, v_R), & t = t_1, x > x_2, \\ (\rho_1, v_1), & t_1 < t < t_2, x = x_2, \\ (\rho_{L*}, v_{L*}), & t \geq t_2, x = x_2. \end{cases} \tag{4.4}$$

According to the boundary value conditions, we can get a unique solution. The large-time behavior of the solution is

$$S_0(U_L, U_{L*}) \to R_1(U_{L*}, U_2) \to R_2(U_2, U_R).$$

Case 1.2:

U_L is between $\check{U}$ and Q. There exists a vacuum. See Figure 14 (right).

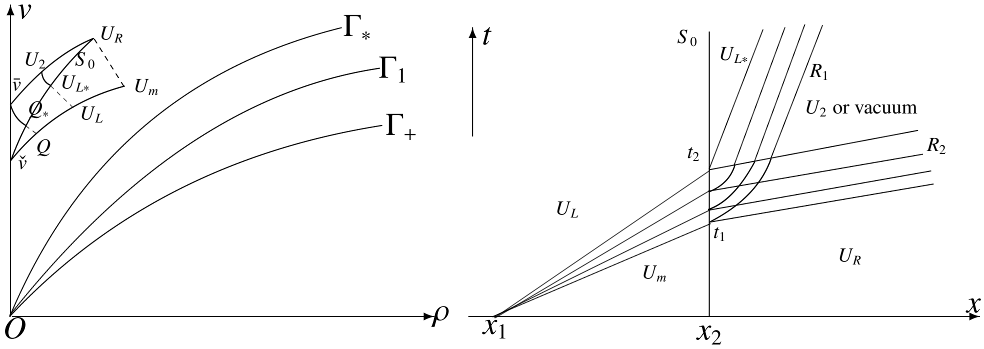

Figure 14. $U_R \in V_1$, U_m is above Γ_1.

Case 2:

$U_R \in V_1$, U_m is below Γ_1. See Figure 13.

Case 2.1:

U_L is between U_m and U_m^s. See Figure 15. This case is similar to Case 1.1, and the solution is

$$S_0(U_L, U_{L*}) \to R_1(U_{L*}, U_2) \to R_2(U_2, U_R).$$

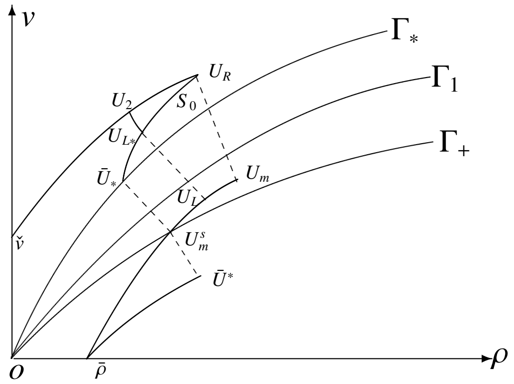

Figure 15. U_L is between U_m and U_m^s.

Case 2.2:

U_L is between U_m^s and $\bar{U}$. See Figure 16. The process of interaction in this case consists of two parts. The first part goes from t_1 to t_2, which is the same process as discussed above. U_0 is between U_m and U_m^s, and $U_1 \in S_0$ is between $\bar{U}_*$ and U_R. In the second part, from t_2 to t_3. $\bar{U}_m \in R_2(U, U_m)$ is between U_m^s and U_L, and $U_1 \in S_0$ is between $\bar{U}_*$ and U_{2*}. The existence and uniqueness of the problem can be obtained by the classical theory from Li [24] and Wang [25]. The large-time behavior of the solution is

$$R_1(U_L, U_2) \to S_0(U_2, U_{2*}) \to R_1(U_{2*}, U_3) \to R_2(U_3, U_R).$$

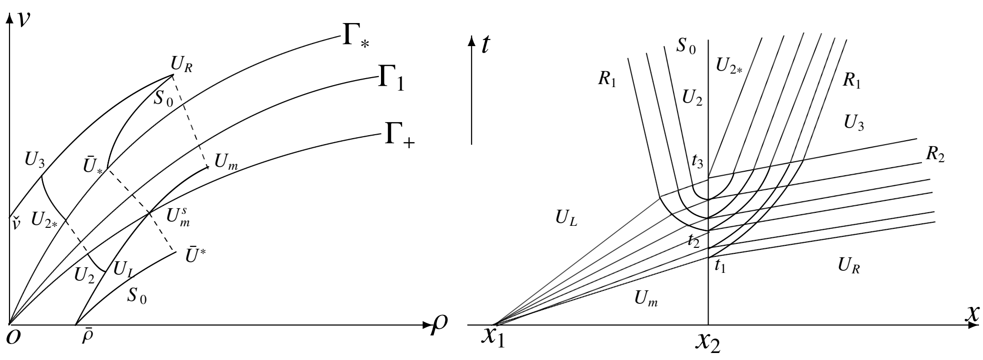

Figure 16. U_L is between U_m^s and $\bar{U}$.

Case 3:

$U_R \in V_4$. See Figure 17. The interaction goes from t_1 to t_2. First, U_L connects with U_2 by $S_1(U_L, U)$. Then, U_2 jumps to U_2^* by the stationary wave, and finally U_2^* reaches U_R by $R_2(U, U_R)$. This process can reflect a backward shock wave. The large-time behavior of the solution is

$$S_1(U_L, U_2) \to S_0(U_2, U_2^*) \to R_2(U_2^*, U_R).$$

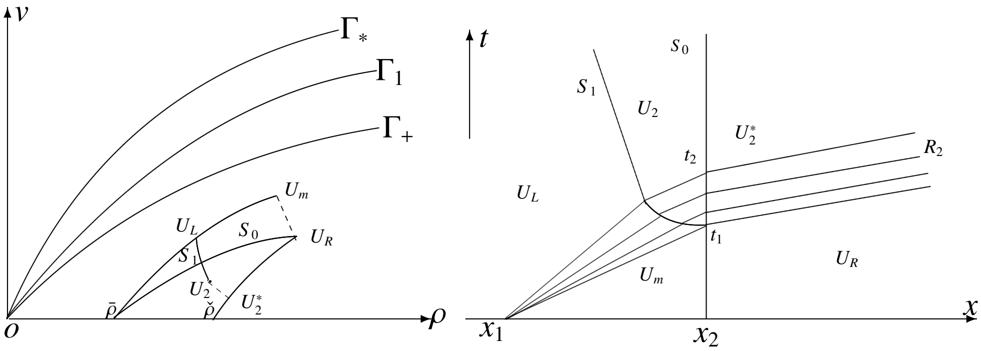

Figure 17. $U_R \in V_4$.

4.2. The interaction of shock wave with stationary wave

We consider the conditions that

$$U_m \in S_2(U_L, U), \quad U_R \in S_0(U_m, U).$$

And we have

$$\begin{cases} S_2(U_L, U_m): \dfrac{v_L - v_m}{\sqrt{(1-v_m^2)(1-v_L^2)}} = \sqrt{\dfrac{(p_L - p_m)(\rho_L - \rho_m)}{(\rho_m + p_m)(\rho_L + p_L)}}, \quad 0 < \rho_m < \rho_L, \\ S_0(U_m, U_R): \begin{cases} (\rho_m + p_m)\dfrac{v_m}{1-v_m^2} = (\rho_R + p_R)\dfrac{v_R}{1-v_R^2}, \\ (\rho_m + p_m)\dfrac{v_m^2}{1-v_m^2} + p_m = (\rho_R + p_R)\dfrac{v_R^2}{1-v_R^2} + p_R. \end{cases} \end{cases}$$

The state $U = (\rho, v) \in S_2(U, U_R)$ is given by

$$\frac{v - v_R}{\sqrt{(1-v_R^2)(1-v^2)}} = -\sqrt{\frac{(p - p_R)(\rho - \rho_R)}{(\rho_R + p_R)(\rho + p)}}, \quad 0 < \rho_R < \rho.$$

Case 1:

U_m and U_R are both located above Γ_+. When $S_2(U_L, U_m)$ overtakes $S_0(U_m, U_R)$, we consider the Riemann problem of (2.1) with

$$(\rho, v, \gamma)\ |_{t=t_1} = \begin{cases} U_L = (\rho_L, v_L, \gamma_L), & x < x_2, \\ U_R = (\rho_R, v_R, \gamma_R), & x > x_2. \end{cases} \tag{4.5}$$

U_{L*} is obtained from U_L by S_0, while the relative position of U_{L*} and $S_2(U, U_R)$ has two subcases.

Case 1.1:

U_{L*} is below $S_2(U, U_R)$. See Figure 18. First, U_L jumps to U_{L*} by the stationary wave, then U_{L*} jumps to U_1 by $R_1(U_{L*}, U)$, and finally U_1 reaches U_R by $S_2(U_1, U_R)$.

The solution in this case is

$$S_0(U_L, U_{L*}) \rightarrow R_1(U_{L*}, U_1) \rightarrow S_2(U_1, U_R).$$

This case indicates that a backward rarefaction wave will be transmitted when the forward shock wave penetrates the stationary wave.

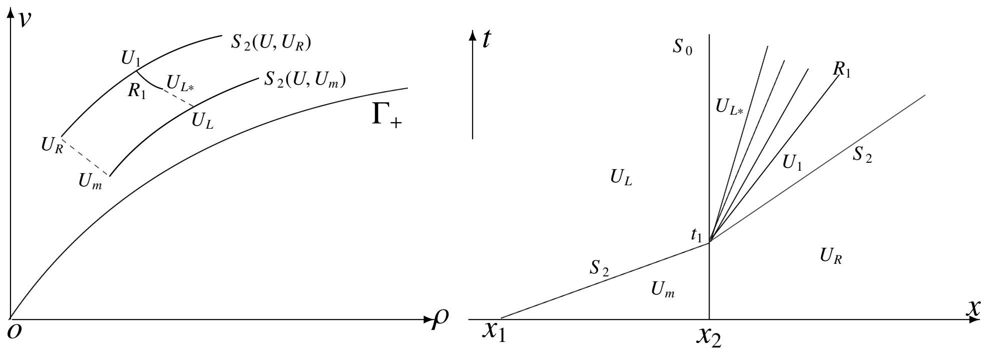

Figure 18. U_{L*} is below $S_2(U, U_R)$.

Case 1.2:

U_{L*} is above $S_2(U, U_R)$. See Figure 19. First, U_L jumps to U_{L*} by the stationary wave, then U_{L*} jumps to U_2 by $S_1(U_{L*}, U)$, and finally U_2 reaches U_R by $S_2(U_2, U_R)$.

The solution in this case is

$$S_0(U_L, U_{L*}) \rightarrow S_1(U_{L*}, U_2) \rightarrow S_2(U_2, U_R).$$

This case indicates that a backward shock wave will be transmitted when the forward shock wave penetrates the stationary wave.

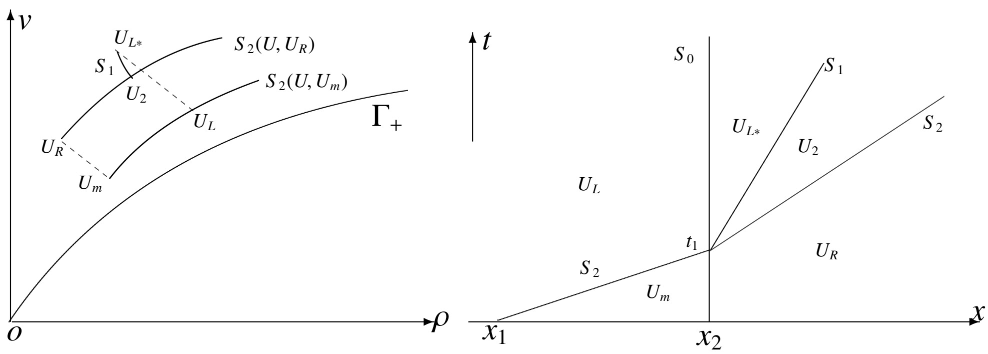

Figure 19. U_{L*} is above $S_2(U, U_R)$.

Case 2:

U_m and U_R are both located below Γ_+ and U_L is below Γ_+. See Figure 20. Similar to Case 1, we discuss the results as follows.

Case 2.1:

U_L^* is above $S_2(U, U_R)$. See Figure 20. U_L jumps to U_3 by $S_1(U_L, U_3)$, then U_3^* is obtained by jumping from U_3 by the stationary wave, and finally U_3^* jumps to U_R by $S_2(U_3^*, U_R)$.

The solution in this case is

$$S_1(U_L, U_3) \to S_0(U_3, U_3^*) \to S_2(U_3^*, U_R).$$

This case indicates that a backward shock wave will be reflected when the forward shock wave penetrates the stationary wave.

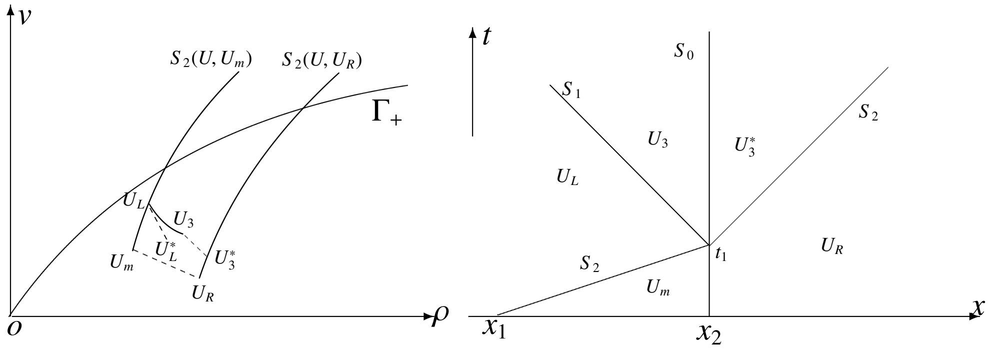

Figure 20. U_L^* is below $S_2(U, U_R)$, U_c^* is above $S_2(U, U_R)$.

Case 2.2:

U_L^* is below $S_2(U, U_R)$. Denote $\{U_c\} = R_1(U_L, U) \cap \Gamma_+$. See Figure 21.

(a) U_c^* is above $S_2(U, U_R)$. See Figure 21. U_L jumps to U_4 by $R_1(U_L, U_4)$, then U_4^* is obtained by jumping from U_4 by the stationary wave, and finally U_4^* jumps to U_R by $S_2(U_4^*, U_R)$.

The solution in this case is

$$R_1(U_L, U_4) \to S_0(U_4, U_4^*) \to S_2(U_4^*, U_R).$$

This case indicates that a backward rarefaction wave will be reflected when the forward shock wave penetrates the stationary wave.

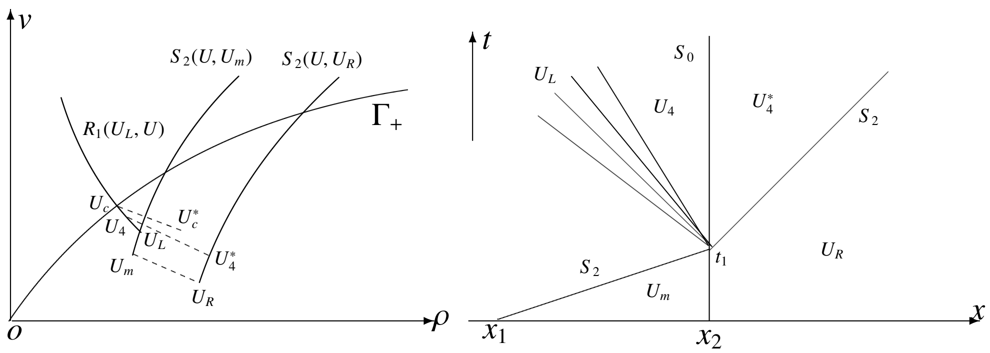

Figure 21. U_L^* is below $S_2(U, U_R)$, and U_c^* is above $S_2(U, U_R)$.

(b) U_c^* is below $S_2(U, U_R)$. See Figure 22. U_L reaches U_c by $R_1(U_L, U_c)$ and U_c jumps to U_{c*} by the stationary wave. Then U_{c*} can jump to U_5 by $S_1(U_{c*}, U_5)$ with $\lambda(U_{c*}, U_5) > 0$ and finally U_5 reaches U_R by $S_2(U_R, U_5)$.

The solution in this case is

$$R_1(U_L, U_c) \to S_0(U_c, U_{c*}) \to S_1(U_{c*}, U_5) \to S_2(U_5, U_R).$$

This case indicates that the forward shock wave will reflect a backward rarefaction wave, which can coincide with the stationary wave, and then transmit a backward shock wave.

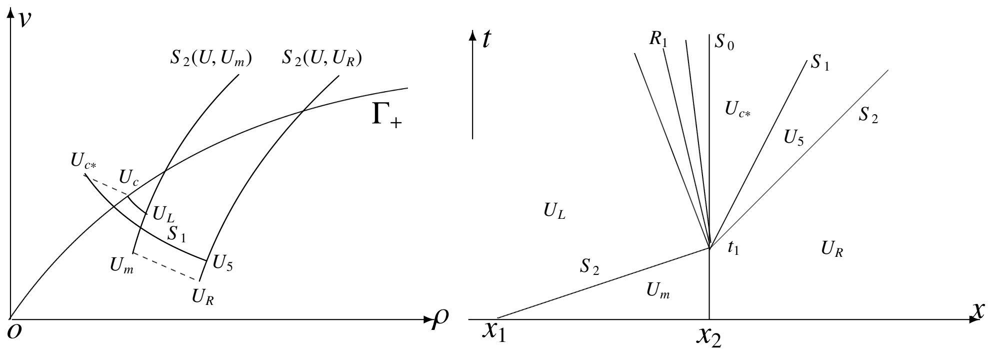

Figure 22. U_L^* is below $S_2(U, U_R)$, U_c^* is below $S_2(U, U_R)$.

Case 3:

U_m, U_R are both located below Γ_+ and U_L is above Γ_+. See Figure 23. We discuss the results as follows.

Case 3.1:

$\tilde{U}_L$ is the state at which the shock speed vanishes, i.e., $\sigma(U_L, \tilde{U}_L) = 0$ and $\tilde{U}_L^*$ is obtained by $S_0(\tilde{U}_L, \tilde{U}_L^*)$. When $\tilde{U}_L^*$ is above $S_2(U, U_R)$, U_L first jumps to U_6 below $\tilde{U}_L$ with $\sigma(U_L, U_6) < 0$, then U_6 jumps to U_6^* by the stationary wave, and finally U_6^* reaches U_R by $S_2(U_6^*, U_R)$. See Figure 23 (left).

The solution in this case is

$$S_1(U_L, U_6) \to S_0(U_6, U_6^*) \to S_2(U_6^*, U_R).$$

This case is similar to Figure 20.

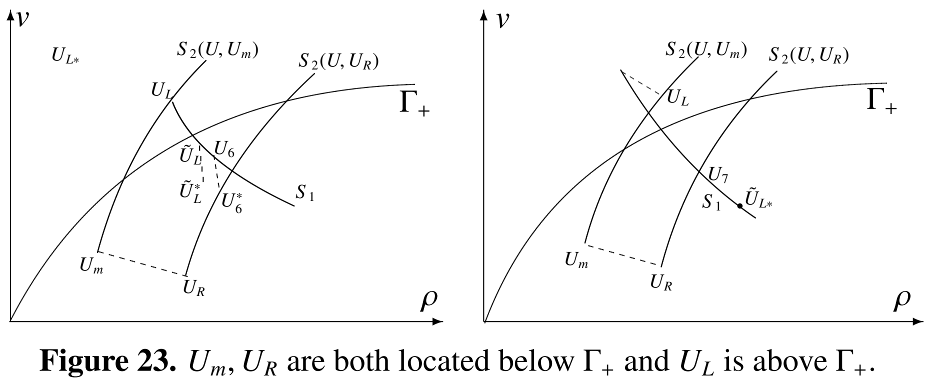

Figure 23. U_m, U_R are both located below Γ_+ and U_L is above Γ_+.

Case 3.2:

U_{L*} is obtained by $S_0(U_L, U_{L*})$ and $\tilde{U}_{L*}$ is the state at which the shock speed vanishes, i.e., $\sigma(U_{L*}, \tilde{U}_{L*}) = 0$. When $\tilde{U}_{L*}$ is below $S_2(U, U_R)$, U_L first jumps to U_{L*} by the stationary wave, then U_{L*} jumps to U_7 above $\tilde{U}_{L*}$ by $S_1(U_{L*}, U_7)$ with $\sigma(U_{L*}, U_7) > 0$, and finally U_7 reaches U_R by $S_2(U_7, U_R)$. See Figure 23 (right).

The solution in this case is

$$S_0(U_L, U_{L*}) \to S_1(U_{L*}, U_7) \to S_2(U_7, U_R).$$

This case is similar to Figure 19.

5. Conclusions

We have solved the Riemann problem for a relativistic p-system with variable heat ratios. The elementary waves including the rarefaction waves, the shock waves, the contact discontinuities, and the stationary waves are derived. The admissible criterion is proposed to select the unique solution across the stationary wave. We also discuss the interaction of elementary waves, especially the rarefaction wave and the shock wave interact with the stationary wave, respectively. The large-time behavior of each case is presented.

Author contributions

Jiatao Yao: Writing - original draft, writing-review & editing, conceptualization, methodology. Qinglong Zhang: Writing-review & editing, conceptualization, funding acquisition. All authors have read and approved the final version of the manuscript for publication.

Use of Generative-AI tools declaration

The authors declare they have not used Artificial Intelligence tools in the creation of this article.

Acknowledgments

This study was supported by the Natural Science Foundation of China (No. 12201323, 12272059) and the Innovation Team Project of Ningbo University (No. 432612623).

Conflict of interest

All authors state no conflicts of interest in this article.

References

1. J. Smoller, B. Temple, Global solutions of the relativistic Euler equations, *Commun. Math. Phys.*, **156** (1993), 67–99. https://doi.org/10.1007/BF02096733

2. J. Chen, Conservation laws for the relativistic P-system, *Commun. Part. Diff. Eq.*, **20** (2007), 1605–1646. https://doi.org/10.1080/03605309508821145
3. A. Taub, Relativistic Rankine-Hugoniot equations, *Phys. Rev.*, **74** (1948), 328. https://doi.org/10.1103/PhysRev.74.328
4. A. Taub, Relativistic hydrodynamics, In: *Hyperbolic equations and waves*, Berlin, Heidelberg: Springer, 1970. https://doi.org/10.1007/978-3-642-87025-5_25
5. K. W. Thompson, The special relativistic shock tube, *J. Fluid Mech.*, **171** (1986), 365–375. https://doi.org/10.1017/S0022112086001489
6. D. Marchesin, P. Paes-Leme, A Riemann problem in gas dynamics with bifurcation, *Comput. Math. Appl.*, **12** (1986), 433–455. https://doi.org/10.1016/0898-1221(86)90173-2
7. M. D. Thanh, The Riemann problem for a nonisentropic fluid in a nozzle with discontinuous cross-sectional area, *SIAM J. Appl. Math.*, **69** (2009), 1501–1519. https://doi.org/10.1137/080724095
8. P. G. LeFloch, M. D. Thanh, The Riemann problem for fluid flows in a nozzle with discontinuous cross-section, *Commun. Math. Sci.*, **1** (2003), 763–797.
9. P. G. LeFloch, M. D. Thanh, The Riemann problem for the shallow water equations with discontinuous topography, *Commun. Math. Sci.*, **5** (2007), 865–885.
10. G. Warnecke, N. Andrianov, On the solution to the Riemann problem for the compressible duct flow, *SIAM J. Appl. Math.*, **64** (2004), 878–901. https://doi.org/10.1137/S0036139903424230
11. N. Andrianov, G. Warnecke, The Riemann problem for the Baer-Nunziato two-phase flow model, *J. Comput. Phys.*, **195** (2004), 434–464. https://doi.org/10.1016/j.jcp.2003.10.006
12. C. H. Hsu, S. S. Lin, T. Makino, On the relativistic Euler equation, *Meth. Appl. Anal.*, **8** (2001), 159–208. https://doi.org/10.4310/MAA.2001.v8.n1.a7
13. G. Q. Chen, Y. Li, Stability of Riemann solutions with large oscillation for the relativistic Euler equations, *J. Differ. Equ.*, **202** (2004), 332–353. https://doi.org/10.1016/j.jde.2004.02.009
14. Y. Li, D. Feng, Z. Wang, Global entropy solutions to the relativistic Euler equations for a class of large initial data, *Z. angew. Math. Phys.*, **56** (2005), 239–253. https://doi.org/10.1007/s00033-005-4118-2
15. B. D. Wissman, Global solutions to the ultra-relativistic Euler equations, *Commun. Math. Phys.*, **306** (2011), 831–851. https://doi.org/10.1007/s00220-011-1299-5
16. G. Lai, Self-similar solutions of the radially symmetric relativistic Euler equations, *Eur. J. Appl. Math.*, **31** (2020), 919–949. https://doi.org/10.1017/S0956792519000317
17. G. Yin, W. Sheng, Delta shocks and vacuum states in vanishing pressure limits of solutions to the relativistic Euler equations for polytropic gases, *J. Math. Anal. Appl.*, **355** (2009), 594–605. https://doi.org/10.1016/j.jmaa.2009.01.075
18. Y. Zhang, H. Yang, Flux-approximation limits of solutions to the relativistic Euler equations for polytropic gas, *J. Math. Anal. Appl.*, **435** (2016), 1160–1182. https://doi.org/10.1016/j.jmaa.2015.11.012
19. Y. Zhang, Y. Pang, Concentration and cavitation in the vanishing pressure limit of solutions to a simplified isentropic relativistic Euler equations, *J. Math. Fluid Mech.*, **23** (2021), 8. https://doi.org/10.1007/s00021-020-00526-2

20. M. Kunik, S. Qamar, G. Warnecke, Second-order accurate kinetic schemes for the ultra- relativistic Euler equations, *J. Comput. Phys.*, **192** (2003), 695–726. https://doi.org/10.1016/j.jcp.2003.07.019
21. K. Wu, H. Tang, A direct Eulerian GRP scheme for spherically symmetric general relativistic hydrodynamics, *SIAM J. Sci. Comput.*, **38** (2016), B458–B489. https://doi.org/10.1137/16M1055657
22. Z. Yang, P. He, H. Tang, A direct Eulerian GRP scheme for relativistic hydrodynamics: one-dimensional case, *J. Comput. Phys.*, **230** (2011), 7964–7987. https://doi.org/10.1016/j.jcp.2011.07.004
23. W. Sheng, Q. Zhang, Interaction of the elementary waves of isentropic flow in a variable cross-section duct, *Commun. Math. Sci.*, **16** (2018), 1659–1684. https://doi.org/10.4310/CMS.2018.v16.n6.a8
24. T. T. Li, Y. J. Peng, The mixed initial-boundary value problem for reducible quasilinear hyperbolic systems with linearly degenerate characteristics, *Nonlinear Anal. Theor.*, **52** (2003), 573–583. https://doi.org/10.1016/S0362-546X(02)00123-2
25. R. H. Wang, Z. Q. Wu, Existence and uniqueness of solutions for some mixed initial boundary value problems of quasilinear hyperbolic systems in two independent variables, *Acta Sci. Natur. Jilin Univ.*, **2** (1963), 459–502.